5-2023

Multiple Output Power Supply using Toroidal Transformers for Medium Voltage Active Gate Drivers

Samhitha Venkata Machireddy
University of Arkansas-Fayetteville

Multiple Output Power Supply using Toroidal Transformers for Medium Voltage Active Gate Drivers

A thesis submitted in partial fulfillment
of the requirements for the degree of
Master of Science in Electrical Engineering

by

Machireddy Venkata Samhitha
GITAM University
Bachelor of Technology in Engineering, 2017

May 2023
University of Arkansas

This thesis is approved for recommendation to the Graduate Council.

_____
H. Alan Mantooth, Ph.D.
Thesis Director

_____
Roy McCann, Ph.D.
Committee Member

_____
Chris Farnell, Ph.D.
Committee Member

ABSTRACT

When operating in high power applications, power devices dissipate tens or hundreds of watts of power in the form of heat. The ability of the power devices to withstand power and dissipation of heat across the power devices becomes a prominent requirement in designing the power converter. This challenge demands a power converter design to be more effective and consistent which factors in size, cost, weight, power density and reliability.

This study aims to propose a gate driver isolated power supply design that can be used in medium voltage applications (e.g., up to 10 kV) while respecting the principle of scalability. A versatile design that facilitates addition of another power switch to the converter if needed, without having to alter too many power supply components while retaining the main structure, thus reducing system complexity and size. The proposed topology is a full-bridge converter with a single-turn primary side transformer, realized using a high voltage insulated hook-up wire as primary winding, while the secondary winding is wound around a toroidal core. This structure can supply several gate drivers simultaneously without replicating the primary side converter, but by simply adding a toroidal core with the secondary side converter which effectively reduces the size of the power supply. To satisfy magnetic and electric constraints, the proposed toroidal transformer needs to exhibit a very low primary to secondary coupling capacitance to avoid high common mode current, which leads to control signal distortion. For this, a multi-objective optimization design has been performed for the magnetic components of the topology. In this paper, a single input and three output power supply design is proposed for a 10 kV active gate driver.

ACKNOWLEDGEMENTS

To begin with, I would like to thank my advisor Dr. H. Alan Mantooth for providing me a great platform to expand my knowledge in the field of power electronics and for his guidance throughout my graduate program. I would like to thank Dr. Roy McCann and Dr. Chris Farnell for being on my advising committee. I would also like to thank the faculty and staff of Department of Electrical Engineering for their support and encouragement through several events.

I would like to thank Xia Du and Yuqi Wei for their extended support through my research work. I'm grateful to be part of the power MSCAD group and I would like to extend my gratitude to my team members Andrea Stratta, Dereje Lemma Woldegiorgis, Liyang Du, Anna Corbitt, Asim Amir Solangi and Zahra Saadatizadeh. I'm thankful for Dr. Chris Farnell and Justin E Jackson for managing the NCREPT (National Center for Reliable Electric Power Transmission) expansion and their guidance through all the testing equipment.

DEDICATION

I would like to dedicate this to my mother, Dr. Sreedevi Kinnera, my sister, Babitha Machireddy and my friends Xia Du, Vasavi Rayachoty and Aashish Pandey for their continuous encouragement and support through this roller coaster journey.

CONTENTS

LIST OF FIGURES

LIST OF TABLES

CHAPTER 1

INTRODUCTION

1.1. Overview

In this day and age where the world is moving towards quick and instantaneous solutions, the demand for high power applications has been increasing. Power modules or power converters are generally used in power supplies, medical equipment, appliances, electric vehicles, and electric motors. Proficient control of power flow in the power converter depends on semiconductor devices and electrical components. Developments in the power electronics field are intended to improve efficiency and reliability of the power devices and power converters. Nevertheless, breakthroughs in materials such as silicon (Si), silicon trench, silicon carbide (SiC), gallium nitride (GaN) also played a vital part in making advancements in power devices.

SiC power devices can sustain higher breakdown voltage and increased thermal capability, thereby supporting higher current density, efficiency, and wider band gap. Comparison of material properties such as thermal conductivity, melting point, electron saturation velocity, energy gap and electric field for the materials Si, SiC, GaN are shown in Figure 1.1 [1] and their respective values are stated in Table 1.

Table 1. Comparison of material properties of Si, SiC, GaN.

Material property	**Si**	**SiC**	**GaN**
Electric Field (V/cm)	$0.3 * 10^6$	$3 * 10^6$	$3.5 * 10^6$
Thermal conductivity (W/cm-℃)	1.5	5	1.3
Melting point (*1000℃)	1.4	2.7	2.5
Electron velocity ($*10^7$ cm/s)	1.0	2.2	2.5
Bandgap (eV)	1.1	3.3	3.4

Materials that need energies higher than one or two electron volts are considered as wide bandgap materials. Wide bandgap devices are used for various purposes such as renewable energy, distributed energy resources and transportation. Wider bandgap materials have higher breakdown voltages, so they can be used to switch large voltages or to switch at higher voltages. Bandgaps of SiC and GaN are exceedingly larger than Si. Therefore, SiC and GaN power devices are more feasible to switch at higher voltages than Si power devices.

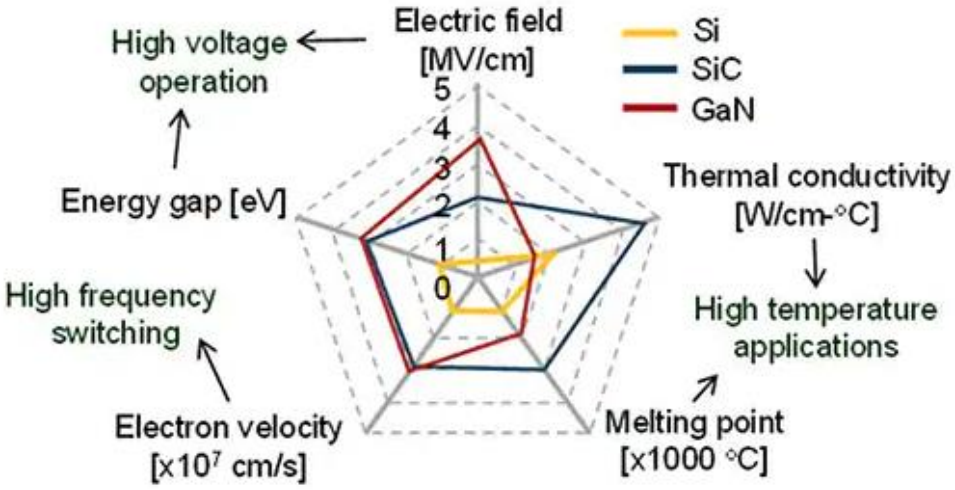

Figure 1.1. Si vs SiC vs GaN material assessment of electrical characteristics. Image is taken from reference [1].

The high electric field of SiC and GaN allows the devices to operate at higher voltages and low leakage currents than Si. Larger electron saturation velocity allows the devices to operate at higher frequency. Si has the lesser electron velocity than SiC and GaN whereas, SiC's electron velocity is slightly lesser than GaN. Hence, GaN devices would be efficient to use at higher frequencies. SiC has higher thermal conductivity than GaN and Si allowing the SiC devices to operate at higher power densities and in high temperature applications. To summarize, SiC has higher melting point, and thermal conductivity whereas GaN has higher electric field. Heat management becomes a challenge to the designer because of the poor thermal conductivity of GaN

devices. When designing a high power module, using SiC devices would be an advantage due to its high electric field, higher thermal conductivity, melting point and wider bandgap.

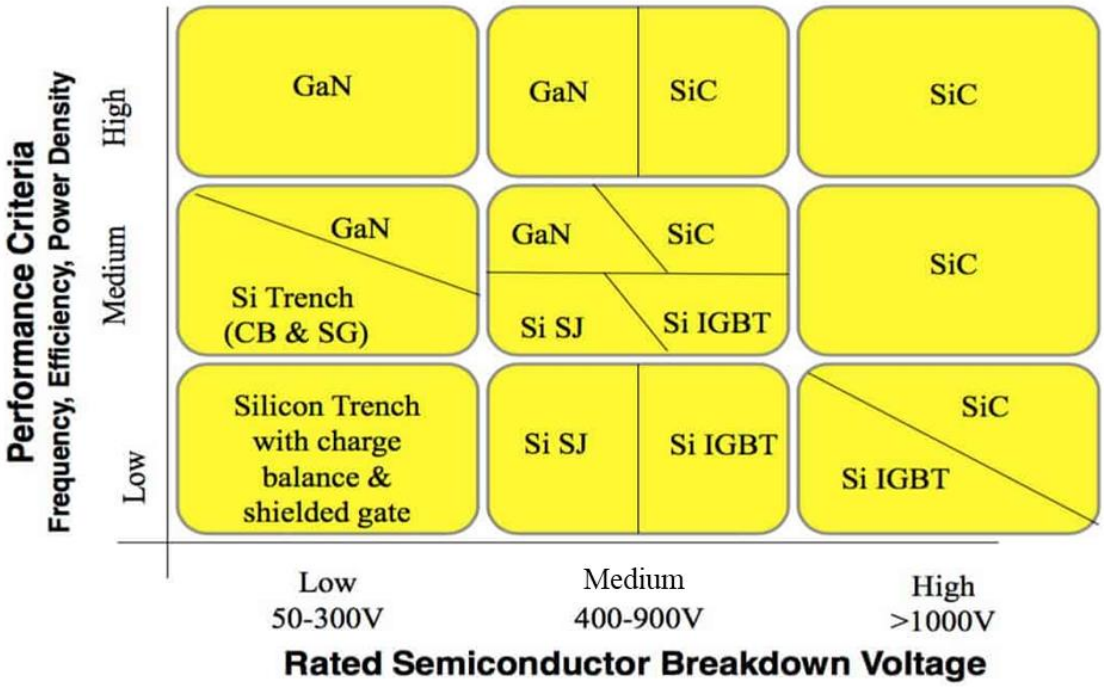

Figure 1.2. Power devices at different rated voltage. Image is taken from reference [2].

Figure 1.2 [2] depicts the correlation between the performance criteria of various power devices and their breakdown voltage, where performance criteria is defined by factoring in operating frequency, efficiency and power density of the power device. Performance criteria has been categorized into three different levels - low, medium, and high. Rated breakdown voltage of the device falls into three different ranges. The low rated breakdown voltage ranges from 50 V – 300 V, medium rated breakdown voltage ranges from 400 V – 900 V and high rated breakdown voltage that has voltages >1000 V. Si trench with charge balance and shielded gate (CG & SG) devices have low range of breakdown voltage whereas the performance ranges from low to medium. GaN devices have low - medium range of breakdown voltage whereas the performance ranges from medium to high. Si super junction (SJ) MOSFET's and Si IGBT (insulated-gate

bipolar transistor) devices have the similar performance criteria; low-medium, however Si IGBT devices have higher rated breakdown voltages than Si SJ devices. SiC devices has higher breakdown voltage and higher performance criteria. To summarize, both SiC and GaN devices have higher performance criteria where GaN devices fall into low rated breakdown voltage and SiC devices fall into high rated breakdown voltage. The selection of a power device depends on the application's rated breakdown voltage, operating frequency, efficiency and power density.

The common topology of a converter circuit consists of many power semiconductors arranged in H-bridge [3] or in pairs of H-bridge configuration. The name H-bridge is derived from its schematic representation. H-bridge configuration connected to a coil is shown in Figure 1.3. where top switches Q1, Q3 are driven by high side gate driver and bottom switches Q2, Q4 are driven by low side gate drivers. When designing a H-bridge converter precaution should be taken so that all 4 four MOSFET's are not to be turned ON or turned OFF at the same time to avoid any abrupt failures. For instance, when MOSFET's Q1, Q4 are turned ON then Q2, Q3 should be turned OFF and vice versa. Necessary dead time and propagation delay should be considered among all the four switches accordingly.

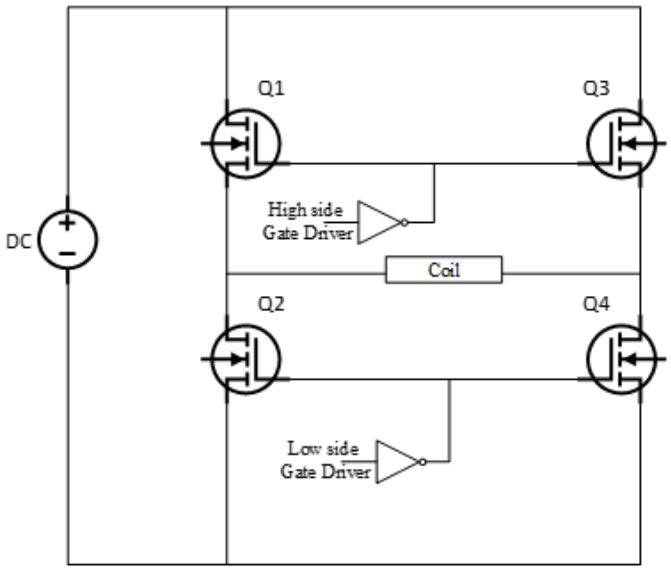

Figure 1.3. H-bridge configuration

The main advantage of the H-bridge circuit is that it is highly efficient with low losses. One of the most important applications of H-bridge circuit is controlling the DC motor driver. Some of the other applications are in robotic technologies, inverter circuits, battery charger for electric vehicles and to regulate speed in different types of drones.

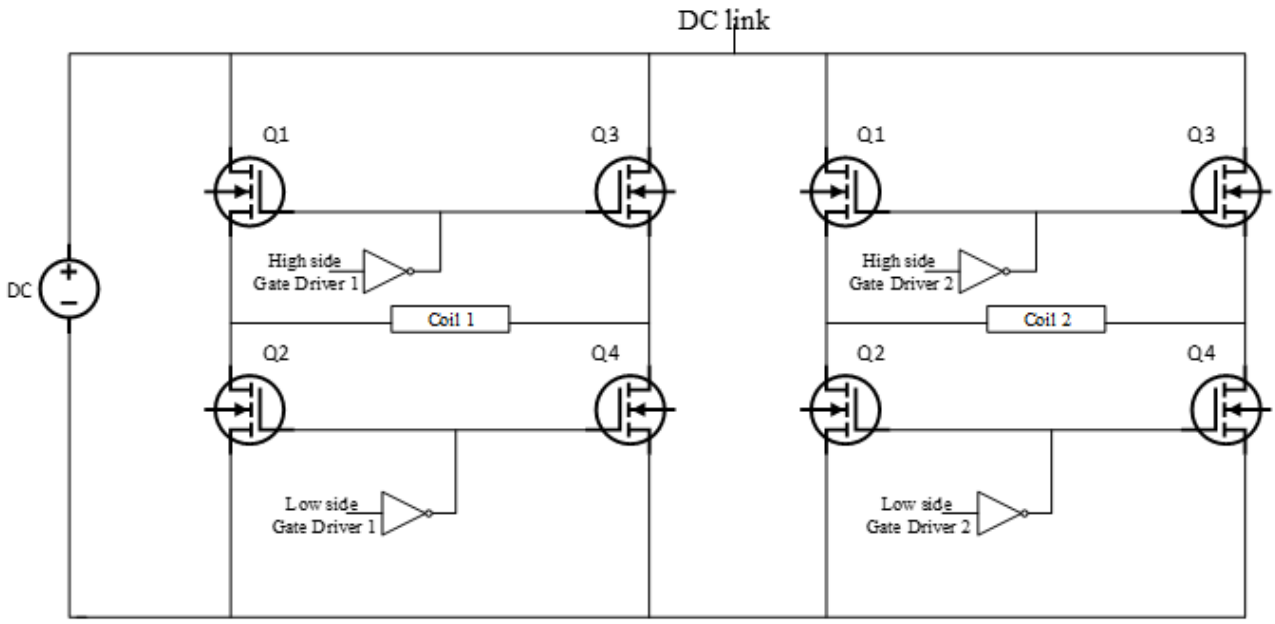

Figure 1.4. Two pair H-bridge configuration

Two pair H-bridge configuration connected parallel to each other [4] is shown in Figure 1.4 where each H-bridge is connected to a coil. Two pair H-bridges are usually used to improve current handling capacity of the circuit.

In the converter circuit, each MOSFET is driven by a gate driver and each gate driver needs a power supply. Designing a medium voltage SiC power converter encounters challenges [3] such as high voltage, high-density and escalation of negative influence on the electromagnetic interference (EMI) noise due to higher switching speed for the gate driver circuit. To mitigate the EMI noise, isolated gate driver power supply also becomes one of the important factors for the gate driver design. When power devices are switching at medium voltages, power supply should

have enough dielectric strength between the power and the control circuits. A review of different gate driver power supplies is illustrated in the next section.

1.2. Thesis organization

This thesis is organized in the following way: different kinds of existing non-isolated switch mode power supplies, isolation techniques and isolated topologies to implement single input and multiple output power supplies are illustrated in Chapter 2. Challenges, design, and simulation of the transformer selection are described in Chapter 3, experimental setup and results are elaborated in Chapter 4 and finally, Chapter 5 concludes the thesis.

CHAPTER 2

BACKGROUND ON SWITCH MODE POWER SUPPLY

Switch mode power supplies have replaced the traditional linear regulator due to its advantages such as higher efficiency, lower power consumption, lower heat dissipation and smaller size [5]. Some applications of these switch mode power supplies are power amplifiers, direct current (DC) motor drives, power stations, personal computers and power industries.

Switch mode power supply uses a semiconductor switching techniques rather than a rectifier to regulate output voltage. Switching regulator can provide step-down, step-up and opposite polarity of the applied input voltage by using different kinds of switch mode circuit topologies such as buck switching regulator, boost switching regulator and buck-boost switching regulator. Buck switching regulator is the power supply that bucks or generates a smaller output voltage than the applied input voltage from the source and boost switching regulator is the type of power supply that boosts or generates a voltage higher than applied input voltage from the source. Whereas a buck-boost switching regulator has a single inductor instead of a transformer and has the flexibility to generate the output voltage higher or lesser than the applied input voltage but with opposite polarity. The magnitude of the output voltage in all three switching regulators can be generated by varying duty cycle of the switching devices like metal oxide semiconductor field effect transistor (MOSFET), bipolar junction transistor (BJT). Buck switching regulator, boost switching regulator and buck-boost switching regulator circuits, their working principles and switching waveforms are discussed in this chapter.

2.1. Asynchronous buck switching regulator

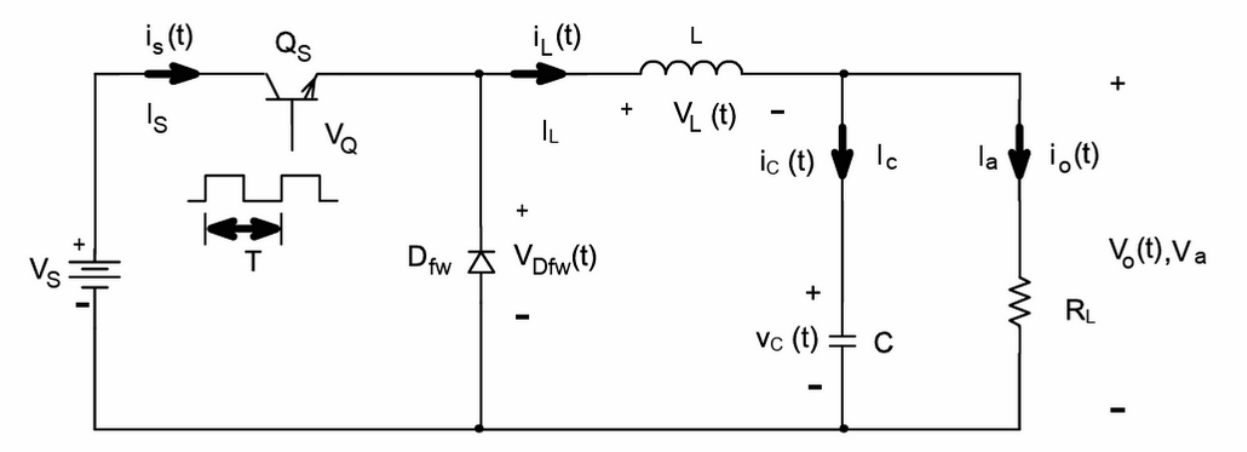

Figure 2.1. Circuit schematic of the asynchronous buck switching regulator. Image is taken from reference [6].

Asynchronous buck switching regulator circuit connection is shown in Figure 2.1 [6]. In this circuit, input voltage or source voltage, Vs is connected in series to the switching device, whereas the input signal of the switching device is given from a control circuit as a pulse width modulation (PWM) signal. The period of one switching cycle has 'turn ON' and 'turn OFF' time. When switching device is turned ON, diode is turned OFF (as it is reverse biased) then the switching device supplies the current to output capacitor, C, through inductor, L, and the inductor starts storing energy as magnetic field, so current across switch, capacitor and inductor starts increasing linearly. When the switching device is turned OFF, the inductor, L, starts releasing the energy stored in it, then current starts flowing into the output capacitor and then to the diode resulting in forward bias or turn ON mode. During this period current across switch is zero as switch is open circuit, so the current across capacitor and inductor starts decreasing linearly. The load resistor receives the current from the output capacitor. The output voltage of the buck converter is the average voltage received at the load resistor. The equivalent buck converter circuit

schematic when the switching device is turned ON and OFF are shown in the Figure 2.2. The output waveforms for the flow of buck switching regulator circuit are shown in Figure 2.3.

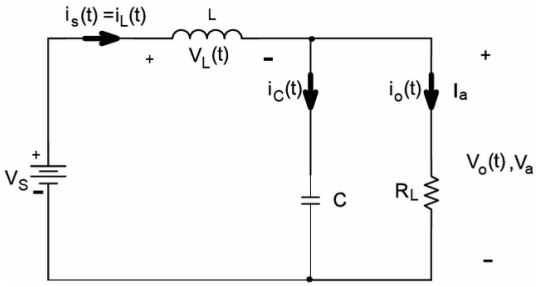

Figure 2.2a

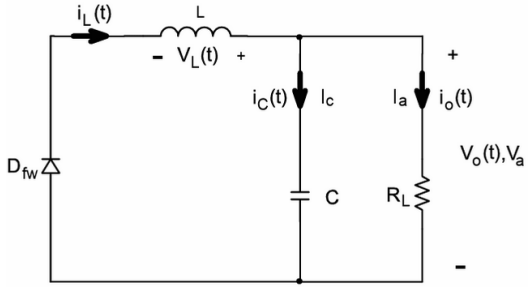

Figure 2.2b

Figure 2.2. Circuit schematic of the asynchronous buck switching regulator circuit schematic when the switching device is turned ON (2.2a) and OFF (2.2b). Image is taken from reference [6].

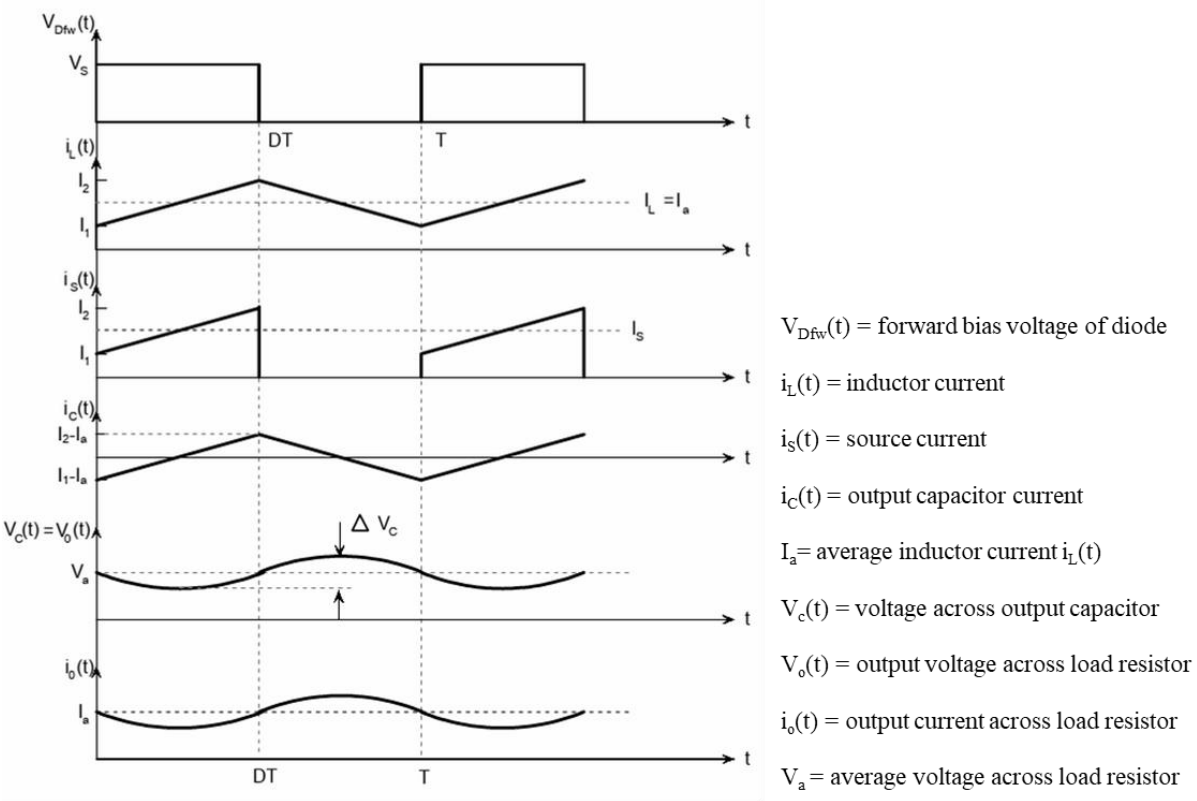

Figure 2.3. Output waveforms for asynchronous buck switching regulator. Image is taken from reference [6].

Considering the switching period of the switching device as T and the duty cycle as D, then the turn ON and turn OFF time cycles of the switching device are as follows:

$$t_{on} = D * T, t_{off} = (1 - D) * T$$

then the average output voltage of the buck switching regulator would be,

$$Va = Vs * D$$

The value of duty cycle is always between 0 and 1 so, the output voltage of the buck switching regulator will always be less than the source voltage.

2.2. Synchronous buck converter

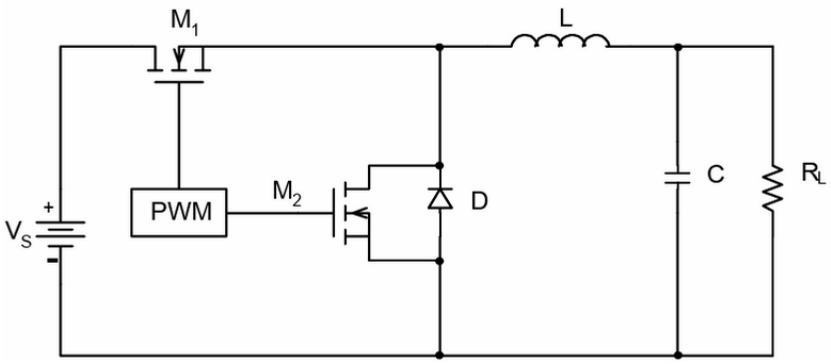

Figure 2.4. Circuit schematic of the synchronous buck switching regulator. Image is taken from reference [6].

When the diode in the asynchronous buck converter is replaced with a switching device like a MOSFET, then it is considered as a synchronous buck switching regulator. The MOSFET's capability for conducting current in both directions provides an advantage over the diode. Among the two MOSFET's, the high side MOSFET is M_1 and the low side MOSFET is M_2. High side MOSFET, M_1 is also referred to as a switching or control MOSFET while the low side MOSFET, M_2 is a synchronous MOSFET. Both the MOSFETs, M_1 and M2 are controlled by their gate signals. The gate signals of the MOSFET's M1 & M2 should be complementary to each other. Even though adding an extra switching device makes the circuit more complex, it is more efficient

than the asynchronous buck switching regulator. One of the main factors to consider while designing a synchronous buck switching regulator is to make sure both the switching devices do not turn ON at the same time, i.e., enough dead time between both the gate signals of the switching devices. If both the MOSFETs turn ON at the same time a short circuit is created from Vs to ground which leads to a destructive misfiring.

2.3. Boost switching regulator

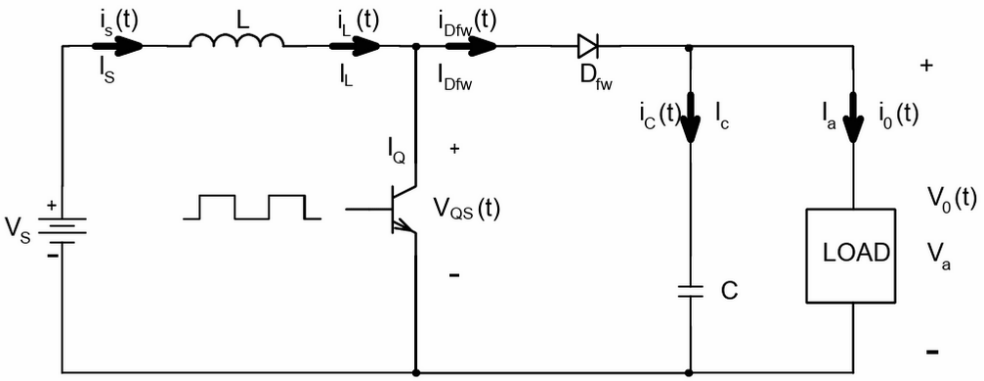

Figure 2.5. Circuit schematic of the boost switching regulator. Image is taken from reference [6].

Boost switching regulator circuit connection is shown in Figure 2.5 [6]. When input voltage is applied from the source, current flows into the inductor and starts storing energy as magnetic field. The input signal of the switching device is given from a control circuit as a PWM signal. The period of one switching cycle has ‘turn ON’ and ‘turn OFF’ time. When the switching device is turned ON, the other end of the switching device is connected to the negative terminal of input voltage. Therefore, there is no current flowing across the diode or the capacitor and so the diode, D is turned OFF. When the switching device is turned OFF, there would be a sudden drop in the current which makes the inductor change its polarity. Since the switching device is turned OFF, current flows into the diode, turning it ON and charging the output capacitor then the current flows to the load. When the switching device is turned ON again, for the next period cycle, the output capacitor starts discharging and supplies current to the load. The load receives current from the

output capacitor. The output voltage of the boost switching regulator is the average voltage received at the load. The equivalent boost switching regulator circuit schematic when the switching device is turned ON and OFF are shown in the Figure 2.6. The output waveforms for the flow of boost switching regulator circuit are shown in the Figure 2.7.

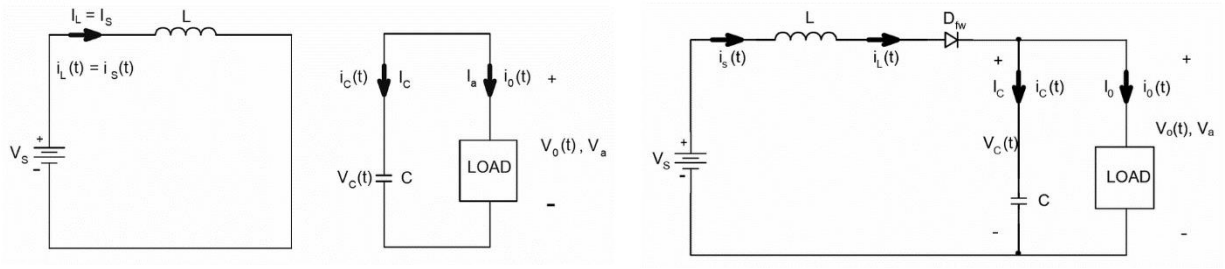

Figure 2.6a Figure 2.6b

Figure 2.6. Circuit schematic of the boost converter when the switching device is turned ON & turned OFF. Image is taken from reference [6].

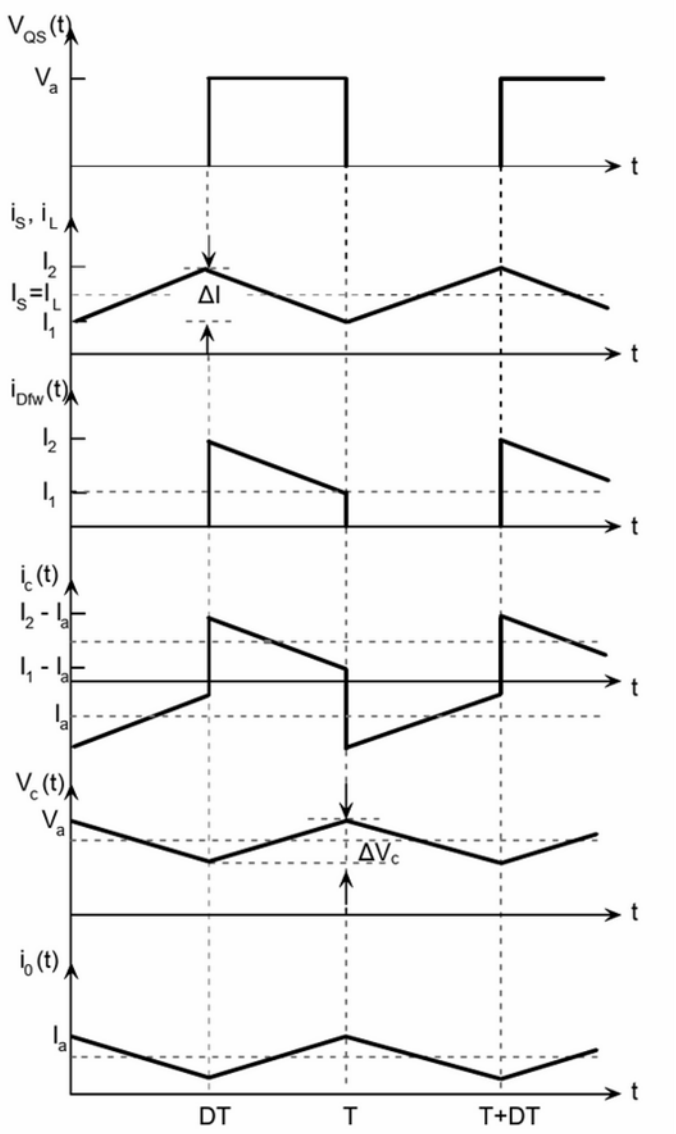

V_{QS} (t) = voltage across transistor

i_L (t) = inductor current

i_S (t) = source current

i_C (t) = output capacitor current

V_c (t) = voltage across output capacitor

i_o (t) = output current across load

V_a = average output voltage across load

Figure 2.7. Output waveforms for boost switching regulator when the switching device is turned ON & OFF. Image is taken from reference [6].

Considering the switching period of the switching device as T and the duty cycle as D, then the turn ON and turn OFF time cycles of the switching device are as follows:

$$t_{on} = D * T, t_{off} = (1 - D) * T$$

then the average output voltage of the boost switching regulator would be,

$$Va = \frac{Vs}{1-D}$$

The value of the duty cycle is always between 0 and 1 so, output voltage of the boost switching regulator circuit will always be greater than the source voltage.

2.4. Buck-boost switching regulator

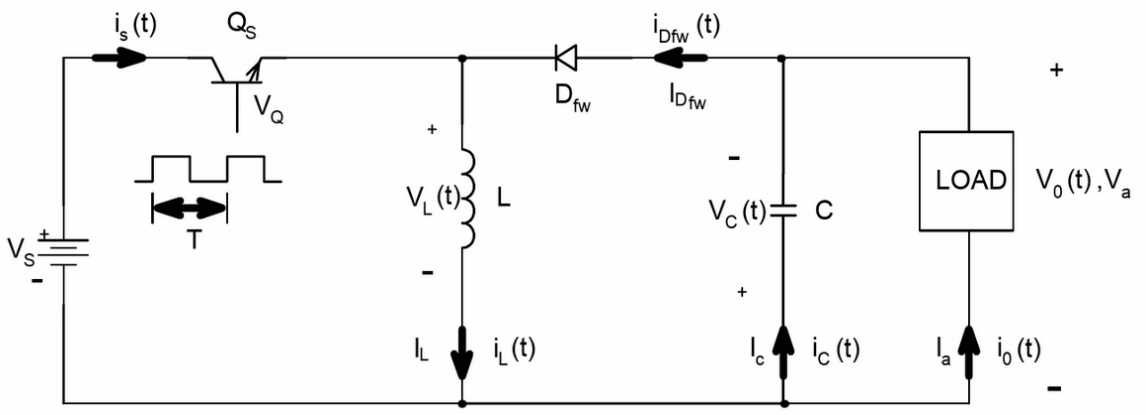

Figure 2.8. Circuit schematic of the buck-boost switching regulator. Image is taken from reference [6].

Buck-boost switching regulator circuit connection is shown in Figure 2.8 [6]. Input voltage is connected in series with the switching device similar to the buck switching regulator circuit. The input signal of the switching device is given from a control circuit as a PWM signal, when the switching device is turned ON, the current will flow from the source voltage to the inductor and the diode is turned OFF (reverse bias). During this cycle, the inductor stores energy as magnetic field. When the switching device is turned OFF, the polarity of the inductor is reversed leading the current into the capacitor and then into the load and the diode (forward bias) is turned ON. The load receives current from the output capacitor. The output voltage of the buck-boost switching regulator is the average voltage received at the load. The output voltage of the buck-boost switching regulator's polarity is opposite to that of the input voltage unlike the buck switching regulator or boost switching regulator. The equivalent buck-boost switching regulator circuit schematic when the switching device is turned ON and OFF are shown in the Figure 2.9. The

output waveforms for the flow of buck-boost switching regulator circuit are shown in the Figure 2.10.

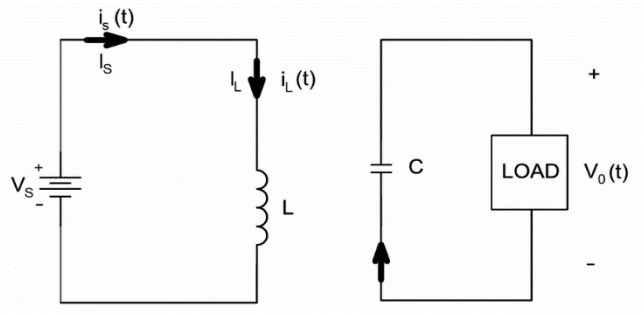

Figure 2.9a

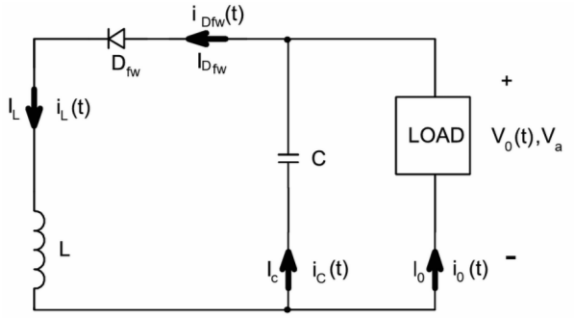

Figure 2.9b

Figure 2.9. Circuit schematic of the buck -boost switching regulator when the switching device is turned ON & OFF. Image is taken from reference [6].

Considering the switching period of the switching device as T and the duty cycle as D, then the turn ON and turn OFF time cycles of the switching device are as follows:

$$t_{on} = D * T, t_{off} = (1 - D) * T$$

The average output voltage of the buck-boost switching regulator would be,

$$Va = \frac{Vs * D}{1 - D}$$

If the value of the duty cycle is between 0 and 0.5, then output voltage, V_a will be less than or equal to source voltage and consequently, the buck-boost switching regulator circuit acts as the buck switching regulator. However, if the duty cycle is between 0.5 and 1, then output voltage, V_a will be greater than or equal to source voltage and consequently, the buck-boost switching regulator circuit acts as the boost switching regulator. However, the downside of using these switching regulators is that they are non-isolated.

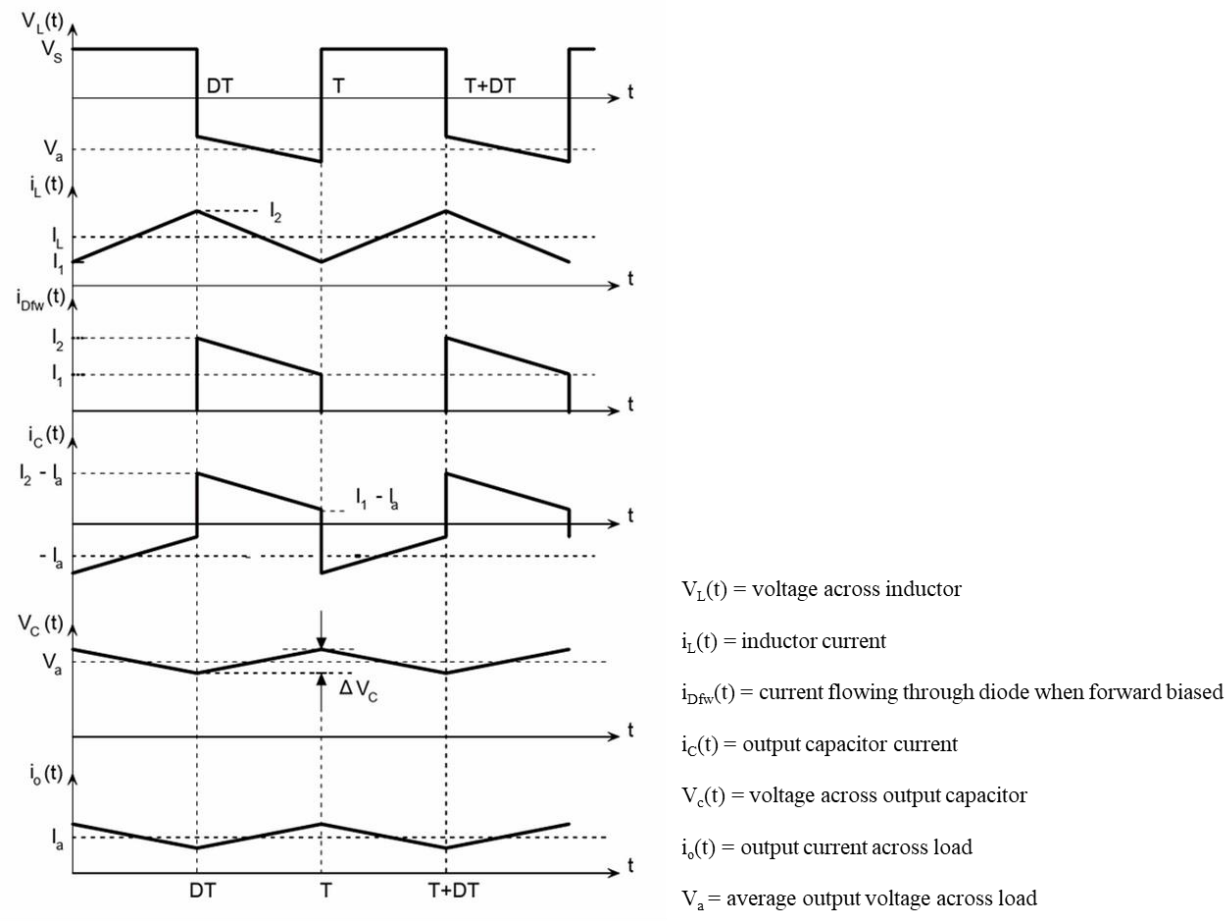

Figure 2.10. Output waveforms for buck-boost switching regulator when the switching device is turned ON & OFF. Image is taken from reference [6].

2.5. Isolated power supplies:

When a circuit is not electrically separated from source to load, it is called as non-isolated circuit. In a non-isolated circuit, operating at low voltages can be quite safe but when there is a high voltage difference between one or more parts of the circuit, there is a high probability for DC currents and some unwanted AC signals to flow which could be very dangerous. In other words, electrical isolation is segregating two circuits to prevent unwanted AC and limiting the DC in a power supply. Also sharing a common ground causes the current flow to damage the input and output supplies while putting the human operator at high risk of electric shock. These risks can be

overcome in the non-isolated circuit by isolating input and output supplies. The schematic and pictorial representation of human risk between the non-isolated and isolated circuit are shown in Figures 2.11 and 2.12 [7].

An isolated circuit is not connected to input and output of the switch mode power supply physically or electrically, this is also referred to as galvanic isolation. Galvanic isolation prevents any flow of electrons between two electrical circuits. In isolated circuits, if there are one or more high voltage circuits then one or more ground loops would be required accordingly. Failure to provide sufficient number of ground loops could cause disruptions or inaccuracies in the system. One of the main advantages of implementing the isolation in an electrical circuit would be removing the surge and grounding problems.

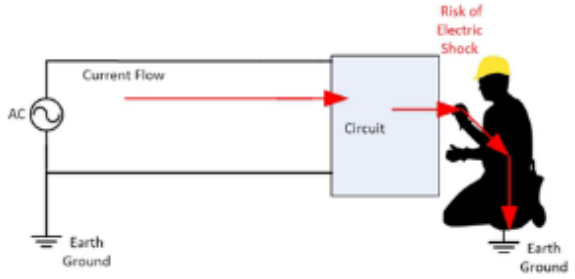

Figure 2.11. Non-isolated power supply. Image is taken from reference [7].

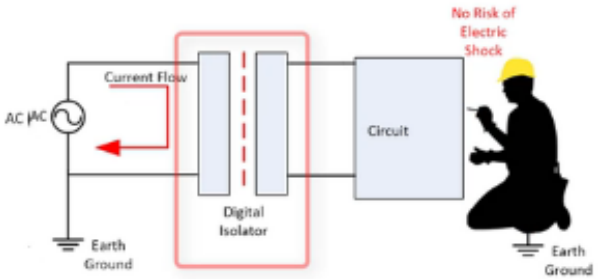

Figure 2.12. Isolated power supply. Image is taken from reference [7].

When a high voltage input is required for a power supply, galvanic isolation is required between the control end and output (where one of it maybe a human operable terminal) with enough safety distance. For example, in electric vehicles a high voltage battery is used to power the drivetrain and this drivetrain is isolated from other low voltage systems by isolating all the sub-systems. However, for internet of things (IoT) devices, isolation may not be required from AC mains, as AC/DC parts of these devices do not have any direct contact with the user end. Therefore, selecting an isolated or non-isolated power supply depends on the application, cost and safety.

Galvanic isolation has a wide variety of applications in medical, electronic industries and communication sector. Medical applications include ECG, endoscopes, defibrillators and imaging devices. Electronic industries applications include measurement systems, I/O logic devices, distribution systems, micro controllers and power generators. Communication sectors include SMPS, routers, chargers and ethernet switches. Isolated and non-isolated power supply have been compared in Table 2.

Table 2. Comparison of non-isolated and isolated power supplies

Non-isolated power supplies	**Isolated power supplies**
Direct current flow between input and output	No direct current flow between input and output
Input and output share the same ground loop	Input and output have their own independent ground loops
Smaller size	Relatively larger size due to addition of isolator between input and output circuits
Dangerous to use in case of a human operator at either end of the power supply	Safe to use when source or load is operated by human
Low cost	Higher price than non-isolated
Higher efficiency	Lower efficiency

Galvanic isolation can be attained by using three technologies; namely optical isolator, inductive isolator and capacitive isolators.

2.5.1. Optical isolator

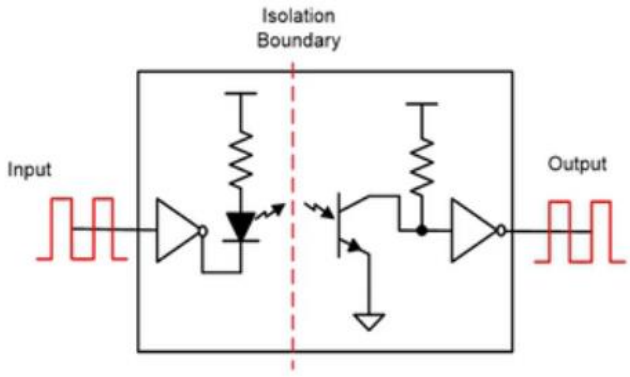

Figure 2.13. Optical isolator. Image is taken from reference [7].

Optical isolators use variable light intensity as a median of communication between the two electrical circuits. Communication through optical isolator consists of a transmitter which emits light waves and a receiver which is a photodetector. Epoxy or mold compounds are typically used as the isolation materials. Example of an optical isolator is shown in Figure 2.13. In the above example, when complementary metallic oxide semiconductor logic is applied it generates current at the input side. Based on the magnitude of input current, light emitting diode (LED) generates a proportional output i.e., higher the input current, higher the intensity of the LED and lower the input current, lower the intensity of the LED. The photodetector, BJT captures the light generated by the LED through the mold compound barrier and generates current at the output side. To isolate both the input and output supplies of the optical isolator, they should have different voltage supplies and ground loops. Another important factor to consider while choosing the optical isolator is rise time and fall time as the change in output is not instantaneous with respect to the change in input. A simple optical isolator "IC – PC-817" is used to show the non-isolated and isolated configurations in Figures 2.14 and 2.15 [8]. The pin diagram of integrated circuit (IC) PC-817 has LED and photo responsive transistor inside the IC. Figures 2.15 shows the schematic of isolated configuration for the IC.

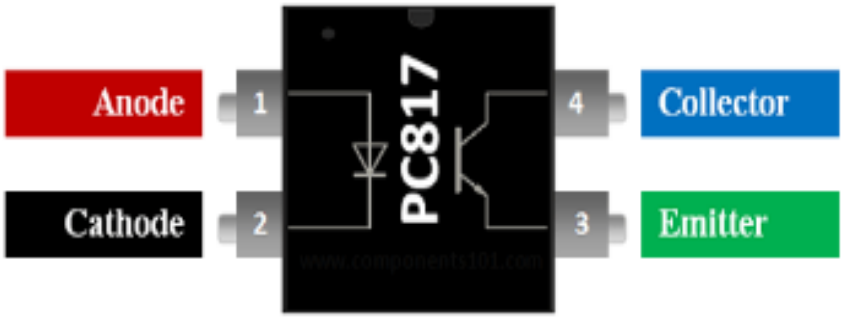

Figure 2.14. Pin diagram of IC - PC817. Image is taken from reference [8].

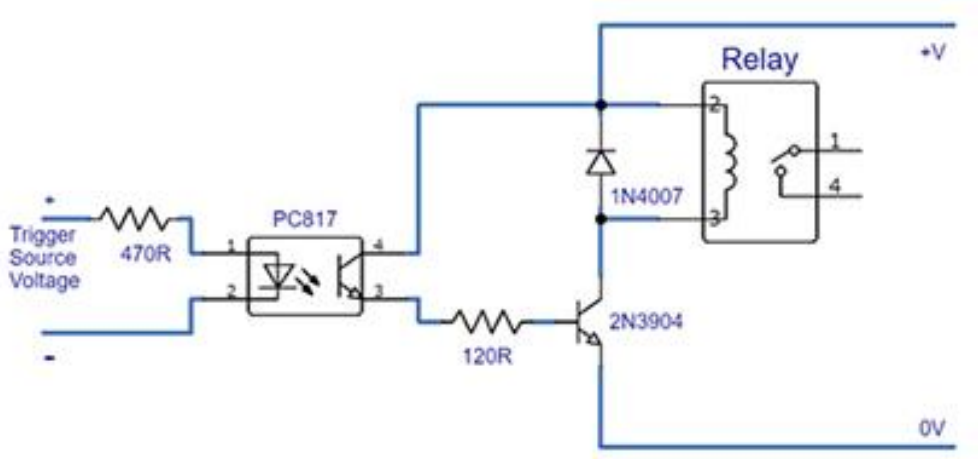

Figure 2.15. IC – PC817 in an isolated configuration. Image is taken from reference [8].

Reliability for this type of isolation can degrade as these devices are affected by aging, varying current gains, and thermal challenges. Some of the applications are microcontroller isolation circuits, signal isolation, AC/DC power control and noise coupling circuits. The signal transfer in the optical isolator is limited to LED switching speed and LED strength tends to diminish over time. These factors contribute to restriction of usage for longer lifetime. Main disadvantage of using the optical isolators is high power dissipation by LEDs.

2.5.2. Inductive isolation

Inductive isolation can be realized by using the coupled inductors. The most common method of inductive isolation is using transformers. Transformers consists of primary winding, secondary winding and core, where primary and secondary windings are wounded up around the core. There is no electrical connection between the input and output side of the circuit. Electrical isolation is achieved by not connecting the primary and secondary windings physically and as a result there is no electrical flow from input to output sides of the circuit. The schematic representation of transformer connections is shown in Figure 2.16.

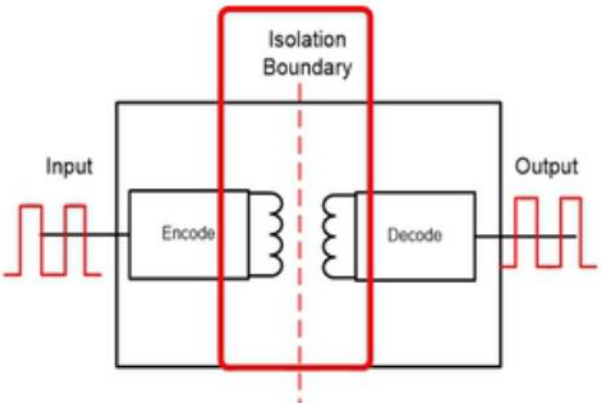

Figure 2.16. Inductive coupling – transformer. Image is taken from reference [7].

When input current passes through the primary winding, it energizes and generates the magnetic flux, known as primary flux. This magnetic flux transmits the energy into secondary winding through electromagnetic induction (EMI) and generates the magnetic flux known as the secondary flux. Transformers are widely used and its frequent applications are stepping up and stepping down voltage. Inductive isolators are used for power isolation. Applications for inductive isolation consists of high voltage alternating current (HVAC) systems, computers, and oscilloscopes.

2.5.3. Capacitive isolation

Capacitors allows the alternating current and prevents the direct current to flow between two points of the circuit. Isolation through this method is provided by designing the capacitive isolators with high dielectric strength. Capacitive isolation is used for power isolation. Arranging a series of capacitors is one way of providing isolation of AC signal. Capacitive isolators are commonly used to avoid failure from a current source. Applications of capacitive isolation comprises of telecom, industrial power, PLC's, and motor drives. Schematic representation of capacitive isolation is shown in the Figure 2.17.

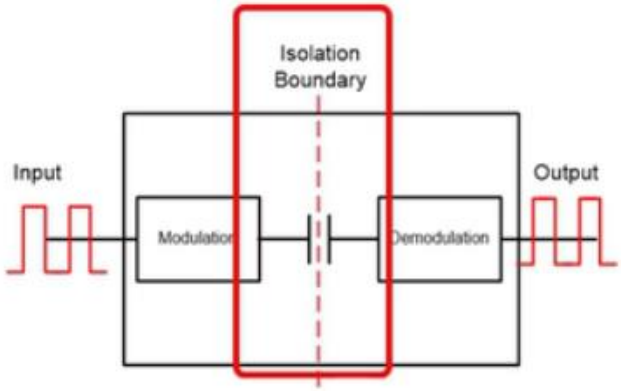

Figure 2.17. Capacitive isolation. Image is taken from reference [7].

The capacitive isolator and inductive isolators provide power isolation, the IC MAX256 is used as an example to illustrate how isolation is obtained in similar application. An example of capacitive isolation using the IC MAX256 are shown in Figure 2.18 [9].

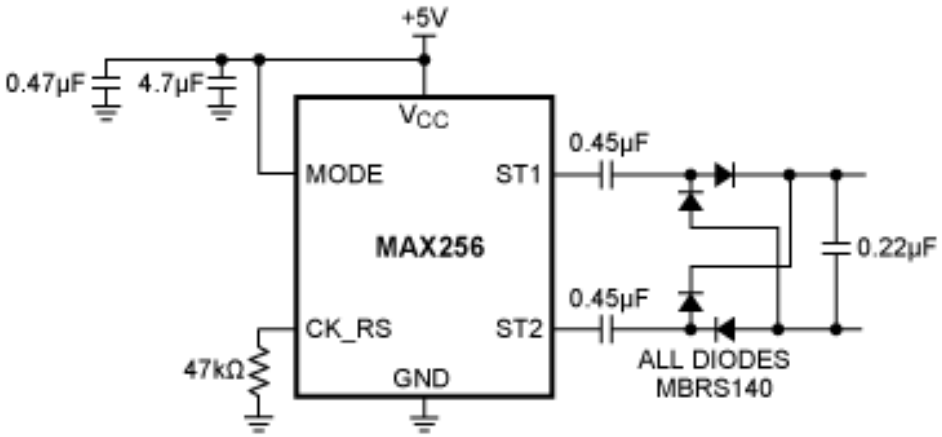

Figure 2.18. Capacitive isolation for IC – MAX256. Image is taken from reference [9].

In Figure 2.18, capacitors, 0.45 uF, provide isolation for the pins ST1 & ST2. ST1 & ST2 signals are connected in series with the capacitors. The signal generated by these capacitors is passed to the output capacitor through the full bridge diode circuit. Schematic of achieving inductive isolation using IC - MAX256 is shown in Figure 2.19 [10].

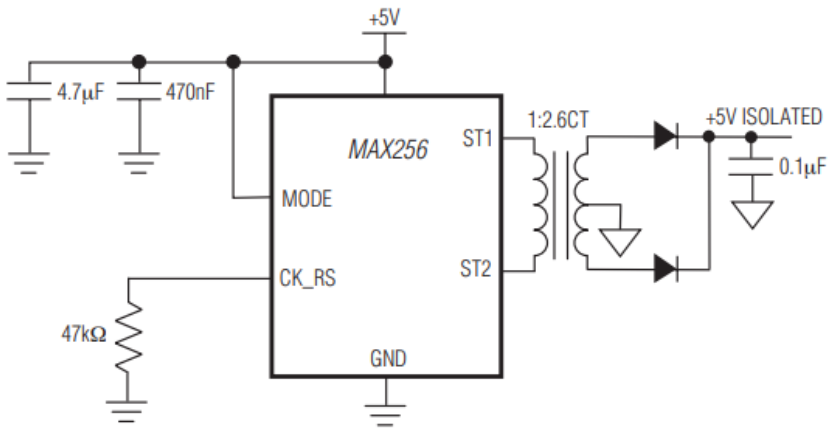

Figure 2.19. Inductive isolation for IC – MAX256. Image is taken from reference [10].

Power isolation and power transfer can also be driven by capacitors when used instead of a transformer. For inductive isolation, transformer is used where pins ST1 & ST2 are the inputs for primary side of the transformer. The signal generated from the secondary winding is passed to the output capacitor through the half bridge diode circuit. The transformer provides isolation for IC – MAX256. In an event of failure, in inductive isolation, the transformer acts as an open circuit whereas, in capacitive isolation, capacitor acts as a short circuit. Using capacitive isolation could be dangerous to the user in failure mode. However, for some applications, capacitive isolation could be favorable when there are limitations on size and cost. Summary of the three types of isolators are described in the Table 3 below.

Table 3. Comparison of the isolators

Optical isolator	**Inductive isolator**	**Capacitive isolator**
Provides signal isolation	Provides power isolation	Provides power isolation
Low speed communications	Higher data rate	High speed communications
Higher power dissipation	Higher the data rate, higher the power consumption	Lower power consumption at high data rates
Cost effective method	Smaller size	Compact size

Commonly used in digital circuits	Commonly used to isolate AC voltages	Commonly used in digital isolators
Resistant to electrical / magnetic noise	Sensitive to electro-magnetic field	Not susceptible to magnetic noise

When the power supply is subjected to high voltage stress in a 10 kV active gate driver, the results might be deleterious in the absence of proper preventive measures. Advantages of inductive isolator such as power isolation, smaller size and open circuit in fault mode outweighs the advantages of optical and capacitive isolators for isolated power supply in medium voltage gate drivers.

2.6. Review of Gate Driver Power Supply Isolation Techniques

Galvanic isolation is a main factor for the gate driver power supply design. With reference to insulation schemes, galvanic isolation can be achieved by either non-transformer-based or transformer-based isolation technique. Non-transformer-based techniques are wireless power transfer (WPT) and power over optic fiber (PoF). Transformer-based techniques are voltage transformer and current transformer. WPT is the more common technique among the core-less transformer-based design techniques, because of the advantage over its fabrication and scalability.

Figure 2.20a. Image is taken from reference [11].

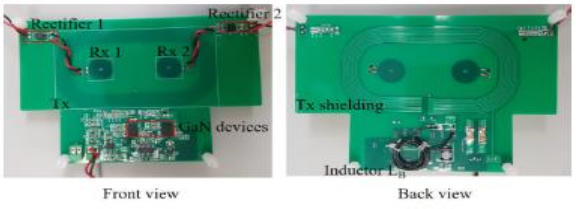

Figure 2.20b. Image is taken from reference [12].

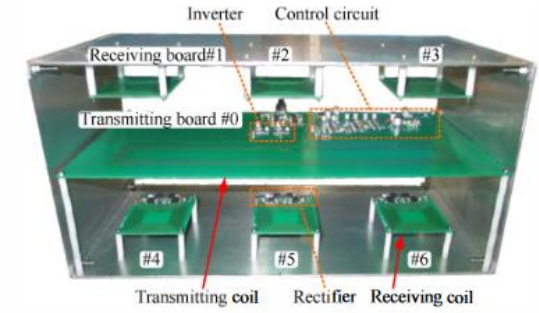

Figure 2.20c. Image is taken from reference [13].

Figure 2. 20. Wireless power transfer systems

Previous studies [11] [12] [13] reported that desired insulation is obtained by placing the primary and secondary coils in the middle of a multi-layer printed circuit boards (PCB) surrounded by the solid insulation as depicted in Figure 2.20. However, the proposed WPTs use air as dielectric material which require larger coils along with longer distance to meet the insulation and power necessities resulting in lower power density. Even though high breakdown voltage is achieved, these structures do not justify the multiple output driving requirements because of their isolated structure.

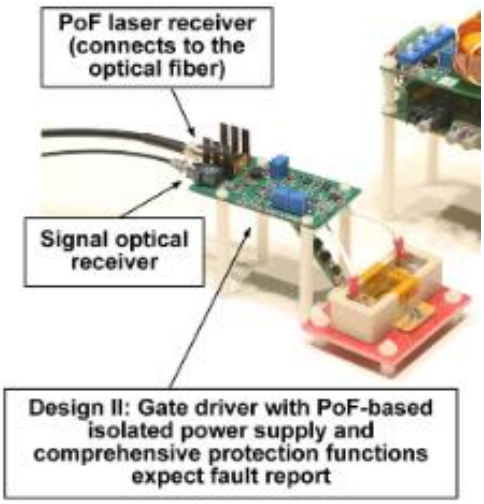

Figure 2.21a. Figure 2.21b.

Figure 2. 21. Power over fiber. Image is taken from reference [14].

The other coreless transformer-based design technique, PoF reported in a study conducted by Zhang et al., [14] as depicted in Figure 2.21, has a negligible coupling capacitance with very high isolation capability (> 20 kV) and has an ability to drive multiple loads. However, the maximum output power is very low (0.5 W), conversion efficiency is < 25 % and its laser transmitter's size is very large which would make it complex to use in medium voltage converters.

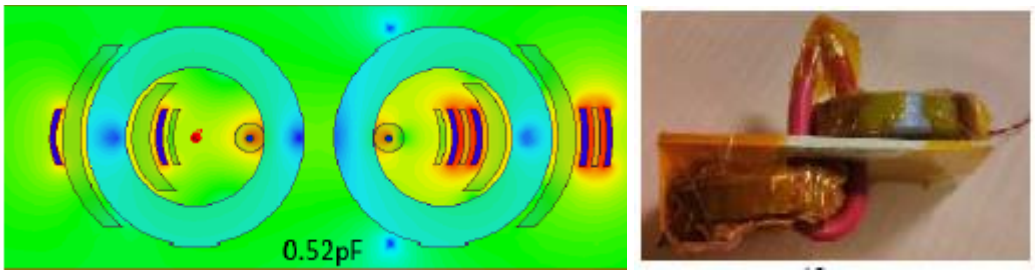

Figure 2. 22. Double galvanic isolated current transformer with coupling capacitance of 0.5 pF. Image is taken from reference [15].

Among the transformer-based design techniques, voltage transformer has good voltage regulation when compared with current transformer. Transformer-based design techniques are more commonly used for high power density systems. In a study based on voltage transformer design by Mainali [15], a double galvanic isolated transformer was used to attain a coupling capacitance of 0.5 pF where two current transformers are connected in series with each other in a proposed medium voltage gate driver as shown in Figure 2.22. Nevertheless, using two magnetic cores for each gate driver leads to a complex design as connecting multiple gate drivers to a single power supply would be more difficult.

Figure 2. 23. Voltage transformer gate driver power supply with silicone gel dielectric material. Image is taken from reference [16].

Zhang et al., [16] proposed a voltage transformer gate driver power supply for medium voltage application, as depicted in Figure 2.23, to achieve a high insulation voltage without increasing the size of the U – shaped voltage transformer, different dielectric materials such as silicone gel, kapton® tape and insulation paper are applied on the transformer and tested. By using the silicone gel dielectric material, this gate driver power supply produced an insulation voltage of 20 kV with an inter-winding capacitance of < 5 pF which is slightly higher than the air insulated design reported by Mainali.

A design with air-insulated single input and multiple output auxiliary power supply is presented in a study conducted by Yan et al.,[17] used a high voltage insulation wire across all the current transformers with a coupling capacitance of 2 pF but has 6 kV of partial discharge voltage and its output voltage is almost half of its input voltage while operating at 1 MHz. A similar single input and multi output auxiliary power supply using high isolation voltage transformers with a coupling capacitance < 3 pF is presented in a study reported by Sen et al.,[18] but with partial discharge voltage of 7.2 k V while operating at 412 kHz. The design reported by Yan et al., insulation is obtained by choosing a material with higher breakdown field and placing the cores in

a 3D printed bobbin and the winding configuration of the power supplies is different as depicted in Figure 2.24.

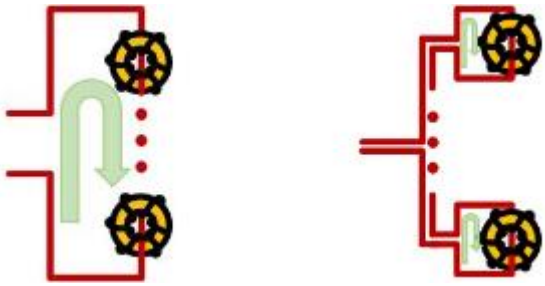

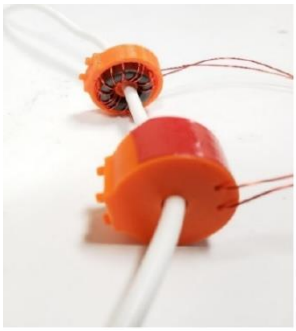

Figure 2.24a. Figure 2.24b.

Image is taken from reference [17]. Image is taken from reference [18].

Figure 2. 24. Winding configuration.

The voltage transformer design is more efficient in voltage regulation than the current transformer. Voltage transformer-based multiple output power supply design is considered.

2.7. Topology selection:

Normally, an isolated topology with multiple secondary windings connected in the transformer can generate multiple output voltages. These circuits utilize only one primary side power stage with multiple secondary power stages. The output voltages are semi-regulated as the precision of generating voltage varies with several factors like inductance coupling among the secondary windings, voltage drop across the rectifiers, parasitic resistances and change in load current. By using the transformer for isolation, there are 3 topologies that could be used to design the single input and multiple output switch mode power supply, namely flyback converter [3], push-pull converter [20] and LLC converter [22].

2.7.1. Flyback converter:

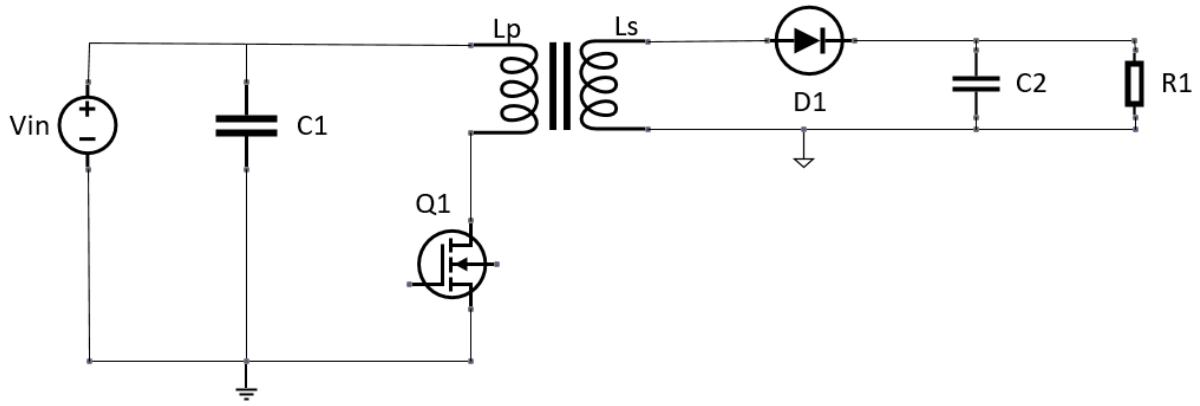

Figure 2.25. Circuit schematic of the flyback converter.

Flyback converters transfer power to output when the switch at primary side is turned OFF. These converters can be used for AC to DC and DC to DC conversion. Schematic of flyback converter is shown in Figure 2.25. Flyback converter circuit primarily consists of input capacitor, switch at the input side, transformer or coupled inductor, output rectifier and output capacitor. Its output can be higher or lower than the applied input voltage. The working principle of flyback converters is primarily based on turn-ON and turn-OFF modes of the primary switch and diode on secondary side. When switch Q at primary side is turned ON and diode D is turned OFF, the input source activates and current starts flowing from input source to the transformer linearly. The transformer stores energy until the switch is turned OFF. During this period, diode is reverse biased and open. Equivalent circuit when the switch is turned ON and diode is turned OFF is shown in Figure 2.26. The red arrows in the Figure 2.26 show the current flow in the circuit when switch is turned ON.

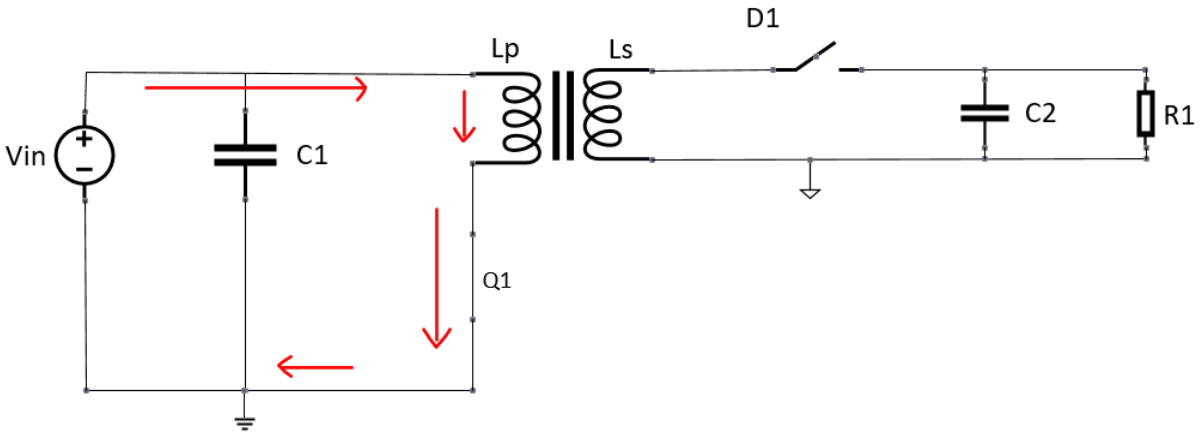

Figure 2.26. Equivalent schematic of flyback converter when switch is turned ON

When switch is turned OFF and diode is turned ON, primary switch is open and secondary diode is short. Current at primary side of transformer is transferred to secondary side and conducts the diode and output capacitor. Then the output capacitor supplies current to the load. Equivalent circuit when switch is turned ON and diode is turned OFF is shown in Figure 2.27. The green arrows in Figure 2.27 represent the flow of current in flyback converter when switch is turned OFF.

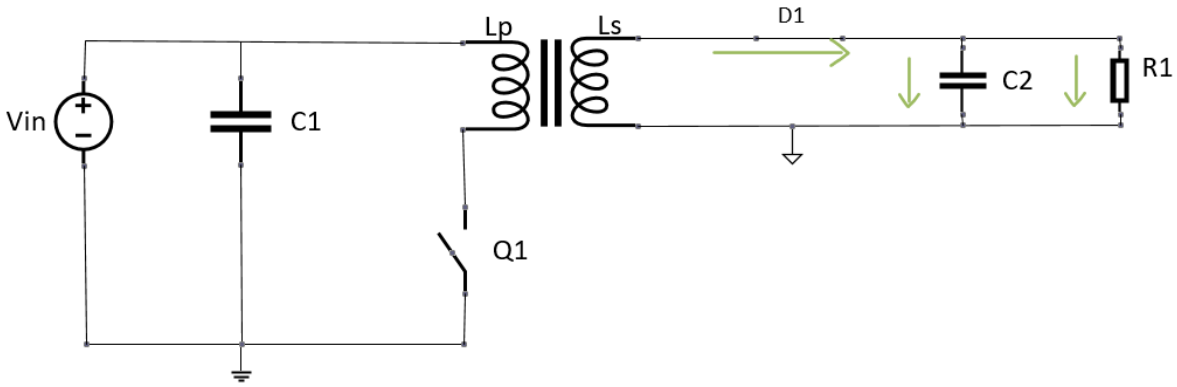

Figure 2. 27. Equivalent circuit of flyback converter when switch is turned OFF

One of the main preventive measure while designing a flyback converter is to not turn ON the switch and diode at the same time to avoid short circuit across the power supply. Flyback topologies are generally used in isolated gate circuits, mobile phones, chargers, standby power supplies in electronic PCs and television sets. Implementing the multiple output power supply design using the flyback converter topology is an easy technique. The output voltages are semi-regulated. LC post-filters can be added to the secondary power stage to reduce the effect of noise.

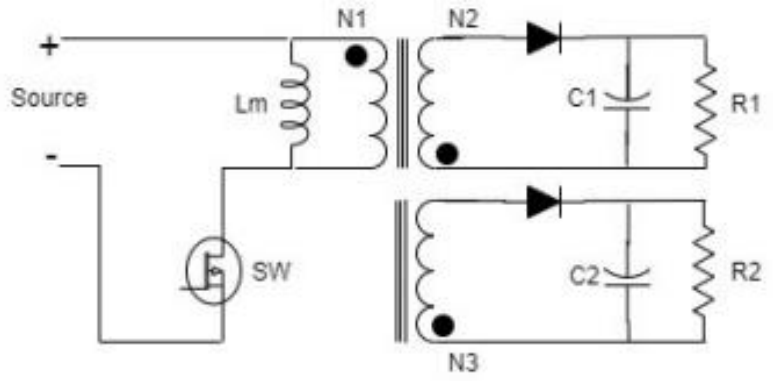

Figure 2.28. Single input and dual output power supply using flyback topology. Image is taken from reference [19].

A closed loop control single input and dual output, as shown in Figure 2.28, was designed in a study reported by Singh et al.,[19] based on flyback topology operating at switching frequency of 10 kHz with 40 % duty cycle where applied input voltage is driven from a photovoltaics supply of 12.6 V to generate output voltages of 23.6 V and 35.9 V.

2.7.2. Push-pull topology:

As the name suggests, push-pull topology defines pushing and pulling the current into and from the transformer. To explain the working principle of the push – pull topology, a simple half bridge push – pull converter is demonstrated as shown in Figure 2.29. In push-pull topology, the transformer is center tapped at both primary and secondary windings, the primary winding has two

parts P1, P2 and secondary winding has two parts S1, S2. Schematic of push-pull converter is shown in Figure 2.29.

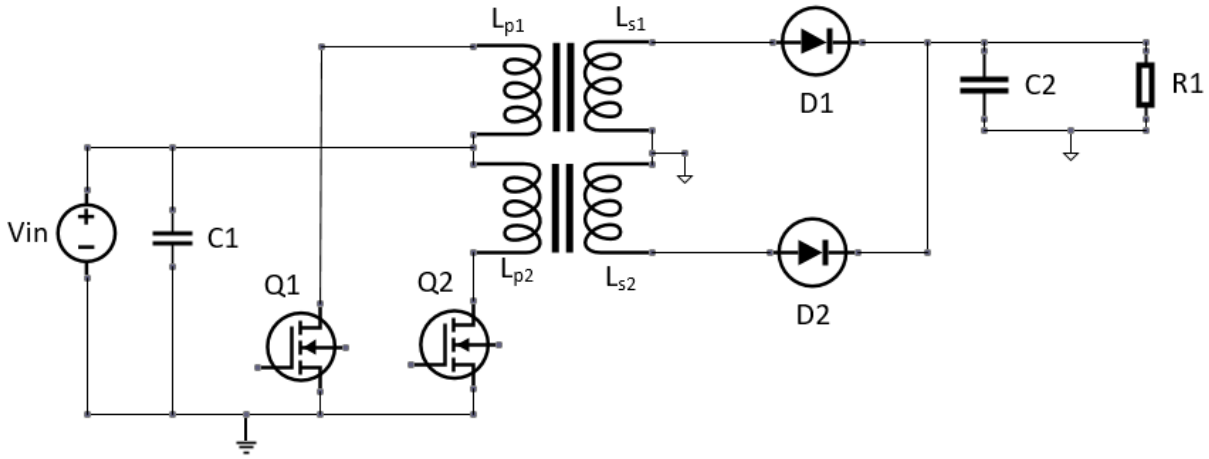

Figure 2.29. Schematic of push-pull converter

The transistors – Q1 and Q2 are operating in alternate switching cycles. Dead time between the switching cycles is required to ensure both the transistors are turned OFF at the same time to avoid short circuiting across the primary power stage. There are three operating modes, first one is when Q1 is turned ON and Q2 is turned OFF, second one is the dead zone where Q1 and Q2 are turned OFF and the last one is when Q1 is turned OFF and Q2 is turned ON. In the first operation mode, when Q1 is turned ON and Q2 is turned OFF, Q1 is short circuited and the input source is activated and current flows through P1 to ground via Q1. Equivalent schematic of push-pull converter when Q1 is turned ON and Q2 is turned OFF is shown in Figure 2.30. Red arrows in Figure 2.30 show the current flow in the circuit when Q1 is turned ON and Q2 is turned OFF.

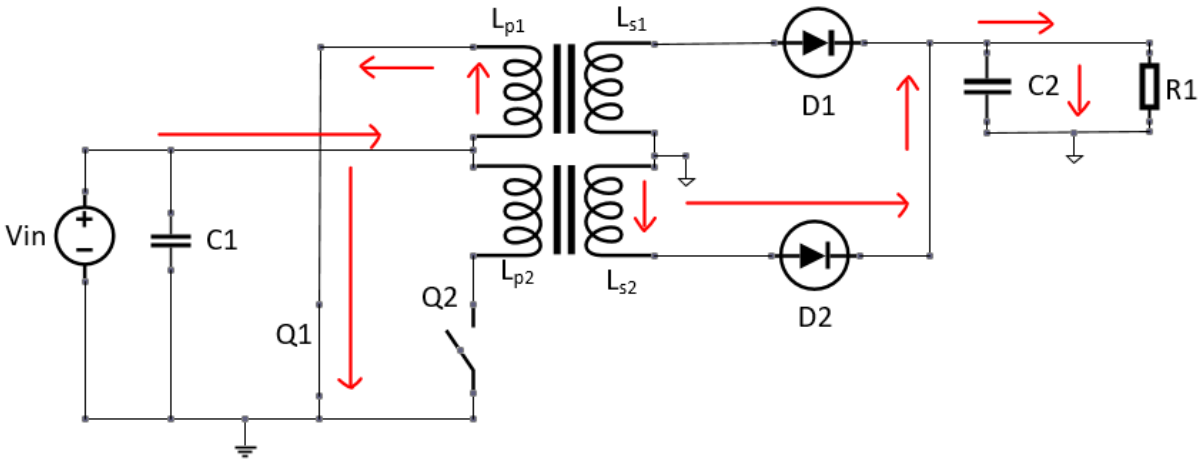

Figure 2.30. Equivalent schematic of push-pull converter when Q1 is turned ON and Q2 is turned OFF.

In dead zone, there is no current flow in the circuit. In the third operating zone when Q1 is turned OFF and Q2 is turned ON, current flows through P2 to ground via Q2. During this period, energy transfers from P1 to S1 then D1 is short circuit and supplies current to the load. Similarly, in the next cycle when Q1 is turned ON and Q2 is turned OFF, energy transfers from P2 to S2 then diode D2 is short circuited then supplies the current to the load. Every time there is a change in current flow, power is transferred from primary circuit to secondary circuit. Equivalent schematic of push-pull converter is shown in Figure 2.31. The green arrows in Figure 2.31 shows current flow in the circuit when Q1 is turned OFF and Q2 is turned ON.

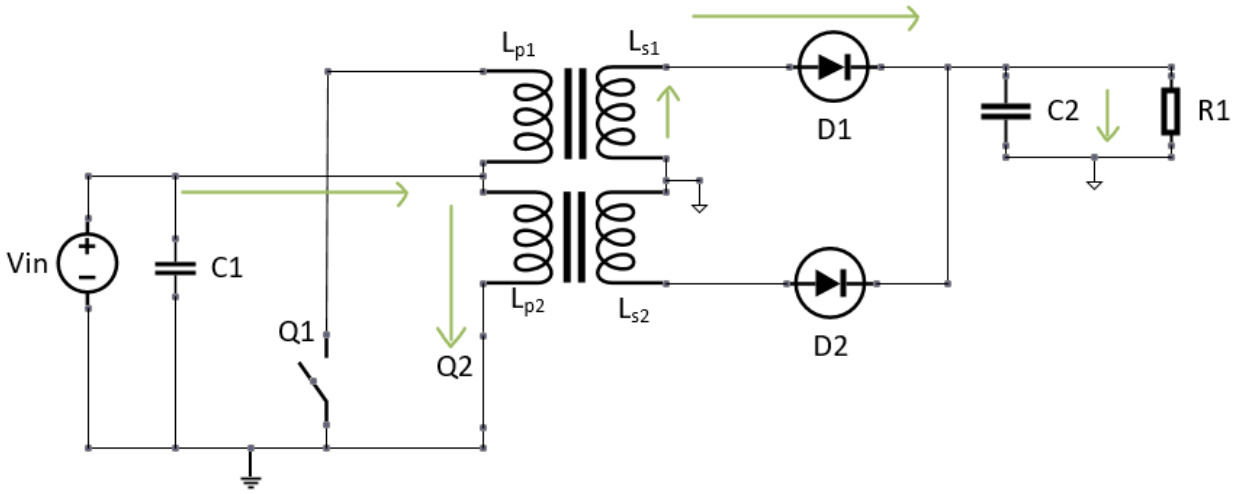

Figure 2.31. Equivalent circuit of push-pull converter in when Q1 is turned OFF and Q2 is turned ON.

Unlike flyback topology, push-pull topology enables power transfer in the entire switching cycle rather than storing energy in one phase of the switching cycle and transferring the energy in another phase of switching cycle. Low EMI is achieved from this topology as primary windings are tightly coupled with each other, flux from primary windings is cancelled out by the secondary windings. A multiple output push-pull converter is implemented in Figure 2.32 [21]. In this study reported by Deepa et al., four isolated outputs are generated using two transformers in parallel connection where each transformer generates two output voltages. Specifications of the converter are as follows; input voltage range is 24 V - 42 V, duty ratio is 45%, switching frequency is 50 kHz and output power is 8 W with an efficiency of 80%. The output voltages are 5 V with 0.5A, 12.5 V with 0.25 A, 12.5 V with 0.1 A and 3.3 V with 0.3 A.

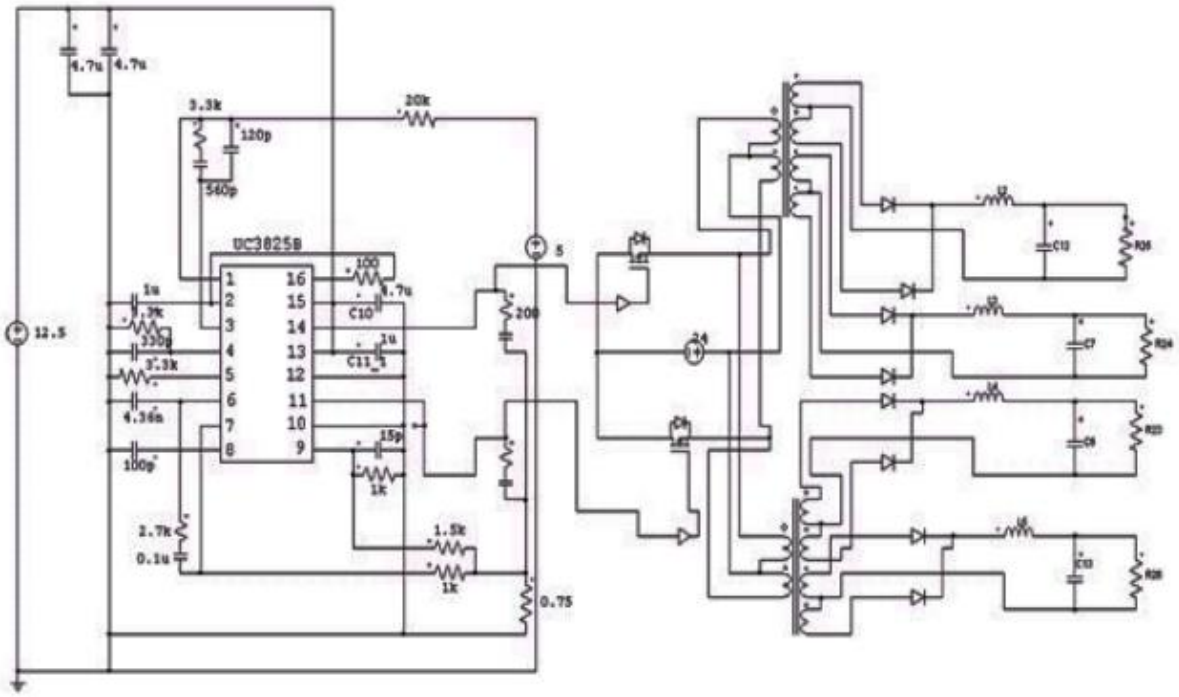

Figure 2.32. Multiple output push-pull converter. Image is taken from reference [21].

2.7.3. LLC topology:

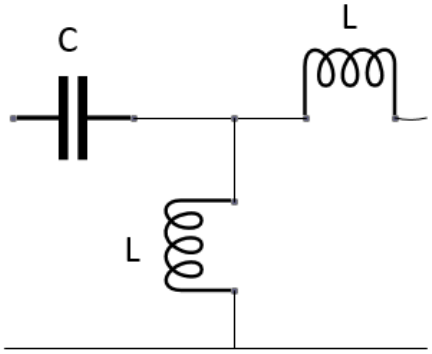

Figure 2.33. LLC resonant tank.

LLC converter topology is part of the resonant converter topologies, which are based on resonant tanks. Resonant tanks are circuits which consists of resistors, capacitors and inductors connected in series or parallel that oscillates at a particular frequency, this frequency is called the resonant frequency. The LLC resonant tank is shown in Figure 2.33. LLC converter can be divided

into four parts- power switches, resonant tank, transformer and rectifier. The schematic of LLC converter is shown in Figure 2.34.

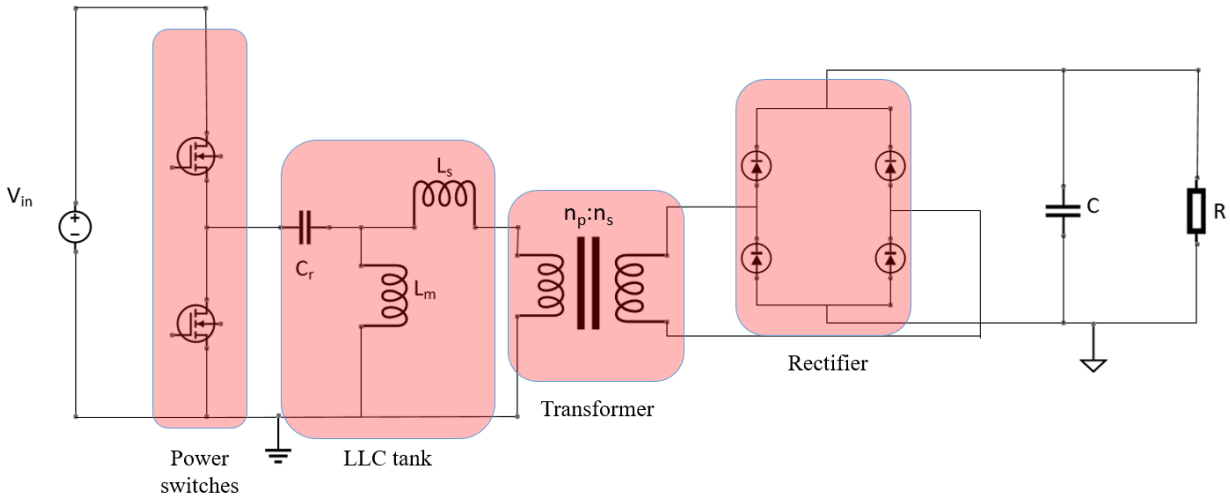

Figure 2.34. Schematic of LLC converter

Power switches are comprised of a half bridge or a full bridge circuit and convert the applied input voltage, DC signal, into a high frequency square wave. Selection of half bridge or full bridge LLC converter is based on the requirements of the application. A full bridge LLC has no off-set value and its peak voltage value is equal to input voltage, whereas the half bridge LLC has half of input voltage as offset value and therefore it has only half the amplitude of the full bridge LLC, as the name suggests. Even though higher number of switches are used for full bridge configuration, lesser number of turns are used reducing the cooper losses and EMI. The high frequency square wave from the power switch is sent to the LLC tank to get rid of the harmonics resulting in a sine wave. Then this sine wave is sent through the transformer where a step-down or step-up phenomena can be performed based on the requirement of the application and finally rectification is performed using the diodes or rectifiers to obtain the DC signal as output. The energy loss in the form of leakage inductance can be compensated by introducing a resonant capacitor. Resonant capacitor can be calculated based on the following equation.

$$f_r = \frac{1}{2\pi\sqrt{LC}}$$

Due to addition of the resonant circuit, LLC converter can achieve high efficiency and enable soft switching at both primary and secondary power stages by minimizing the switching losses. In contrast to flyback converter, there is no need for a LC past filter at the output and therefore it saves board space and cost. A two output DC-DC converter is implemented by Wei et al., [23] using half bridge LLC topology, its schematic is shown in Figure 2.35.

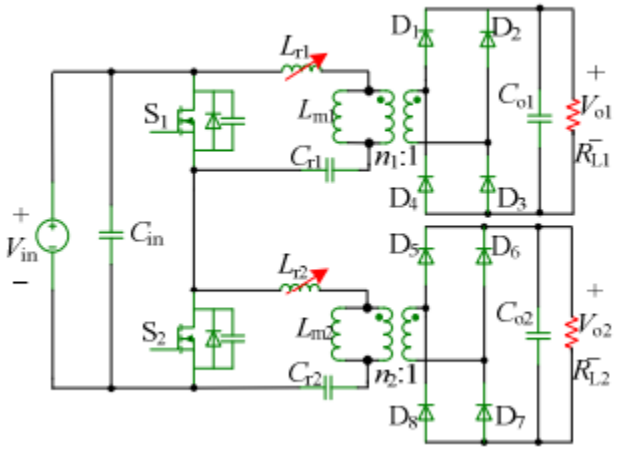

Figure 2.35. Dual output DC-DC converter. Image is taken from reference [23].

Design specifications of the dual output DC-DC converter are input voltage ranges from 300 V to 380 V, output voltages are 24 V and 48 V and operating at 100 kHz. For the implemented topology, there is no cross regulation issue between outputs and both the outputs are regulated independently.

2.8. Proposed power supply design

Isolated gate drivers play a prominent role in power converters. Isolated gate drivers consists of one or more complementary transistors, they draw low voltage from the power supply and convert it into a higher voltage to supply the gate terminal of power switch in the power

converter. Therefore, isolated power supplies are required to design an isolated gate driver. In Figure 2.36, a schematic representation of a proposed active gate driver for medium voltage power modules with paralleling operation structure is seen where parallel connection of transistors are driven by high side and low side isolated active gate drivers. These active gate drivers are driven by isolated gate driver power supplies.

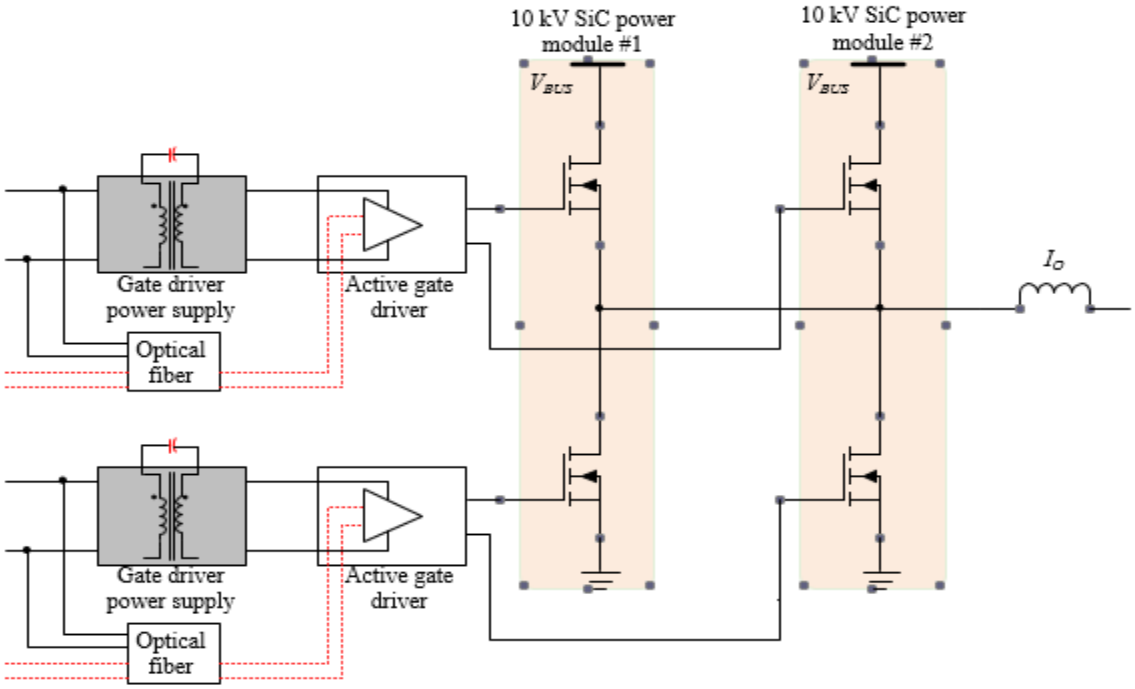

Figure 2.36. Proposed active gate driver for medium voltage power modules with paralleling operation

Even though using a transformer as an isolation barrier has a lot of advantages, factors such as parasitics, leakage inductance and inter-winding capacitance has a negative influence on transformer efficiency.

Flyback converter is commonly used for applications involving gate driver power supplies. However, leakage inductance of the flyback converter affects the efficiency of power transfer and coupled inductors [21] which generates voltage spikes across the converter might damage the

system. This can be overcome by choosing the LLC topology, as addition of resonant tank reduces the effect of leakage inductance across the transformer. Consequently, efficiency of power conversion is higher than the flyback converter. Therefore, LLC converter is the better choice to design an isolated power supply for the isolated gate drivers.

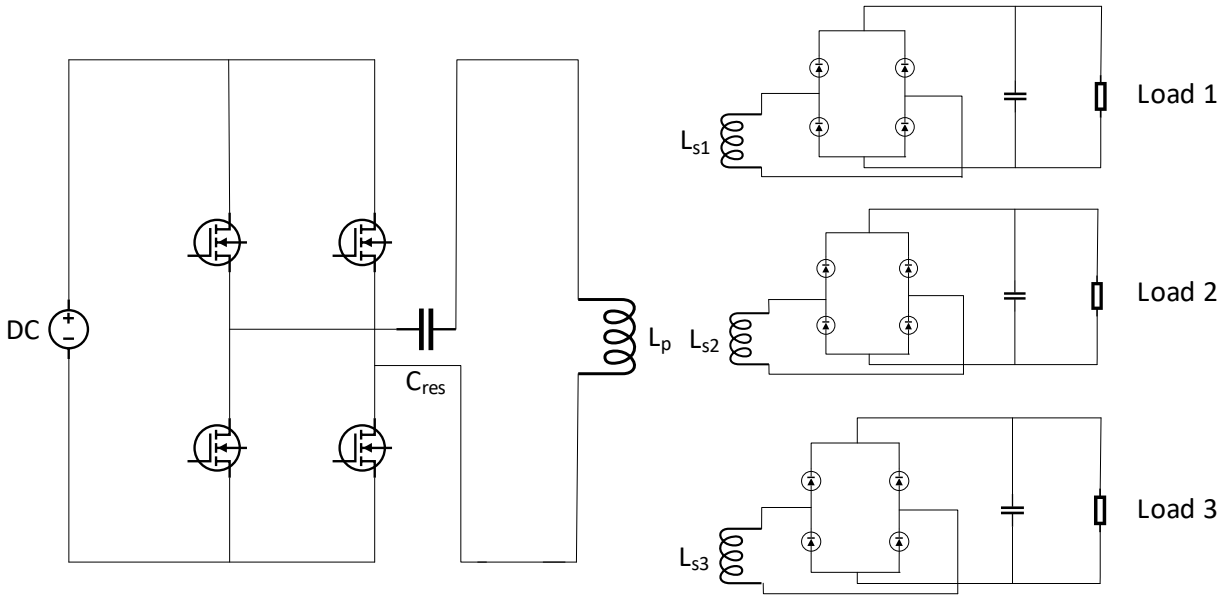

Figure 2.37. Proposed power supply for the multiple output power supply design

The proposed power supply for the multiple output power supply design as shown in Figure 2.37 is the full bridge circuit connected to the single turn primary winding. Multiple secondary windings would be used to generate output to drive the multiple gate drivers of the power modules. The input voltage or direct current voltage, V_{in} would be connected in parallel to an input capacitor, C_{in} and full bridge configuration. A resonant capacitor, C_r is connected in between the positive terminal of the full bridge configuration and the positive terminal of the single turn primary winding. The isolated transformer would be connected in such a way that the single turn primary winding, high voltage insulated hook up wire, would be passed through the toroidal core and connected to the output of the full bridge configuration whereas the secondary winding would be winded-up around the toroidal core as seen in Figure 2.38.

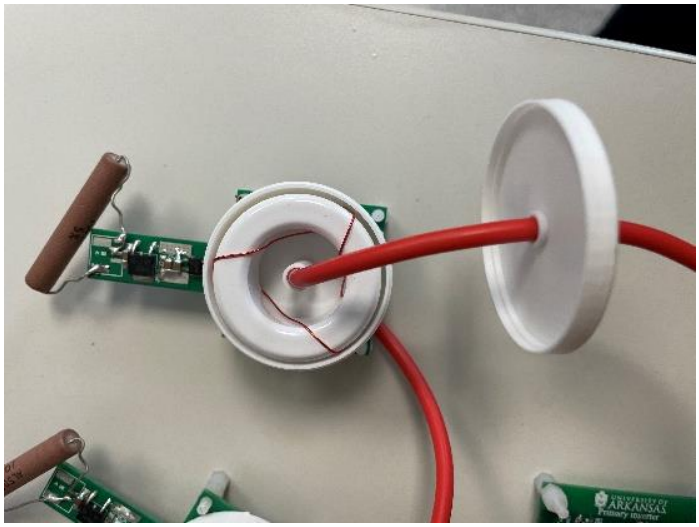

Figure 2.38. Proposed single turn toroid transformer

The output of secondary winding of the toroidal core, AC voltage, would be connected to the full bridge rectifier circuit to rectify the AC output voltage of the secondary winding and then the voltage regulator will regulate the output voltage into DC voltage. Analysis of the circuit was performed in the LTSPICE simulation software. The output voltage waveform of one of the output is shown in Figure 2.39.

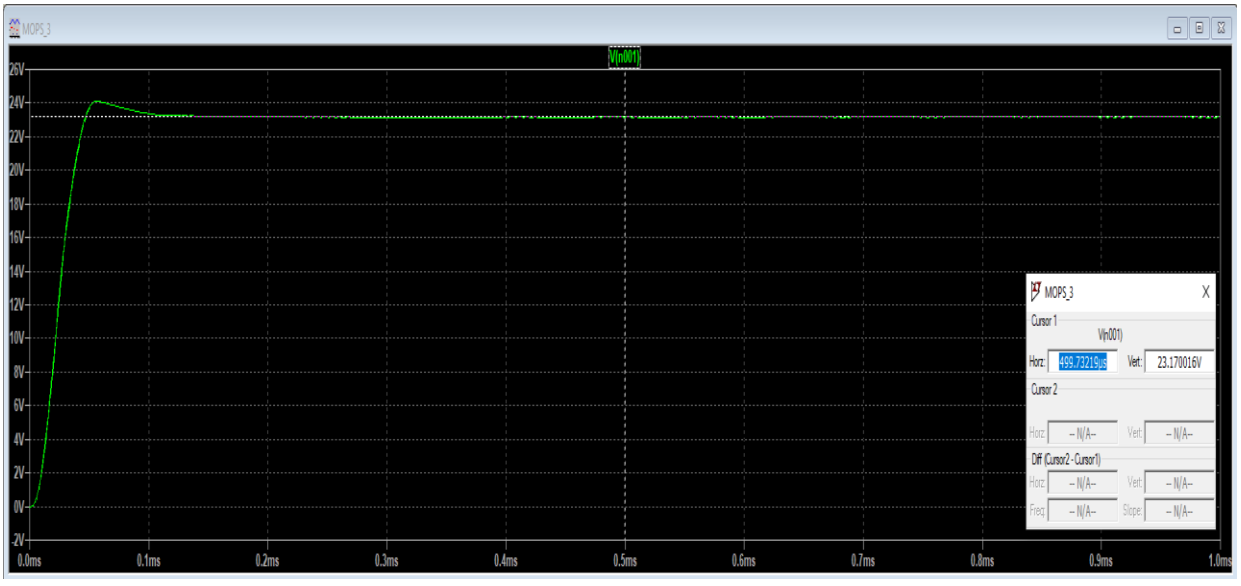

Figure 2.39. Output voltage waveform of the power supply

Design specifications of the single input and multiple output power supply are shown in the Table 4 below.

Table 4. Specifications of the multiple output power supply

Parameter	**Symbol**	**Value**
Input voltage	V_{in}	20 V
Output voltage	V_{out}	23.14 V
Resonant capacitor	C_{res}	34.938 nF
Switching frequency	f_{sw}	500 kHz

CHAPTER 3

DESIGN OF TRANSFORMER

3.1. Introduction to transformers

A transformer can be used to transfer the voltage or current from the primary side circuit to secondary side circuit. The basic structure of a transformer consists of a core, a primary winding and a secondary winding. Coils are wound around the core as shown in Figure 3.1 [24].

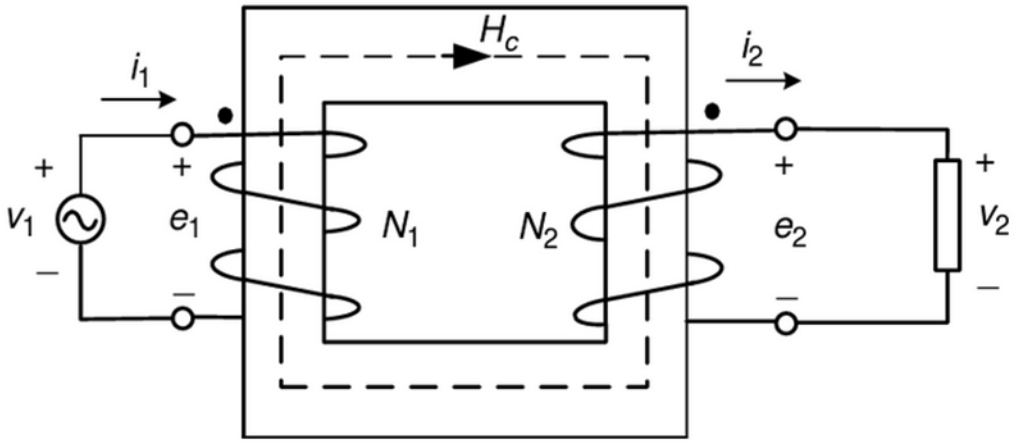

V_1 = alternating voltage applied to the primary side
i_1 = current entering into the primary winding
e_1 = electromagnetic flux (EMF) induced at primary winding
N_1 = number of turns at primary winding
V_2 = alternating voltage applied to the secondary side
i_2 = current entering into the secondary winding
e_2 = EMF induced at secondary winding
N_2 = number of turns at secondary winding

Figure 3.1. Structure of a transformer. Image is taken from reference [24].

A transformer has two or more mutually coupled windings. When an alternating voltage is applied to the primary winding, a resultant flux is generated over the primary winding based on the number of turns in the primary winding. The flux generated also depends on the magnetic material of the core, air-gap of the core, physical dimensions of the core and cross sectional area

of the windings on the core. The magnetic flux generated over the primary winding is transferred to the secondary winding and then to the load. An ideal transformer can transfer all the magnetic flux generated from the primary side to the secondary side. However, due to phenomena such as leakage inductance, mutual inductance, core losses, eddy current losses there is some energy loss in practical transformers.

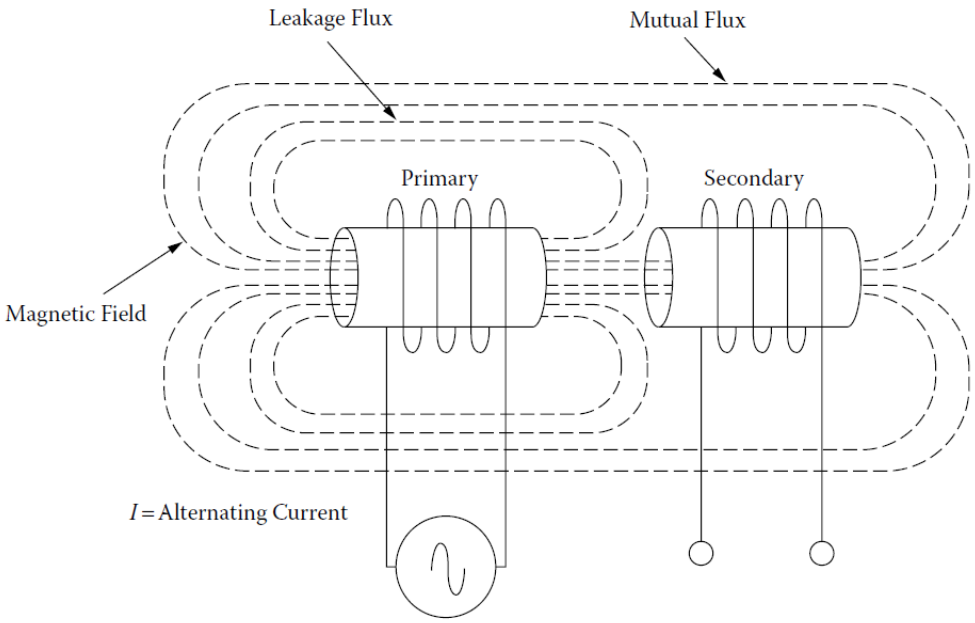

Figure 3.2. Magnetizing and leakage flux in transformer. Image is taken from reference [25].

In Figure 3.2 [25], primary winding is connected to an alternating current source and secondary winding is open circuited. The dotted lines indicate the magnetic field generated at the primary and secondary windings. Magnetic flux is defined as the quantity of magnetic field passing through a given surface. The magnetic flux generated by the primary winding is not same as the magnetic flux generated at the secondary winding. The magnetic flux that is common in both primary winding and secondary winding is called mutual flux and the magnetic flux that is not excited to the secondary winding is leakage flux. The mutual flux and leakage flux are indicated

by inductances. Mutual flux is indicated by magnetizing inductance, M and leakage flux is indicated by leakage inductance, L_s. They can be calculated by the following equations,

$$L_S = L_1 - \frac{M^2}{L_2}; M = k\sqrt{(L_1 L_2)}$$

where L_1 and L_2 are the self-inductances of the primary and secondary windings respectively, k is the coupling co-efficient of the transformer.

For an ideal transformer, coupling co-efficient is always 1 whereas for a practical transformer, it is always between 0 and 1. The equivalent circuit of a practical transformer upon considering the mutual and leakage flux is as shown in Figure 3.3. [25]

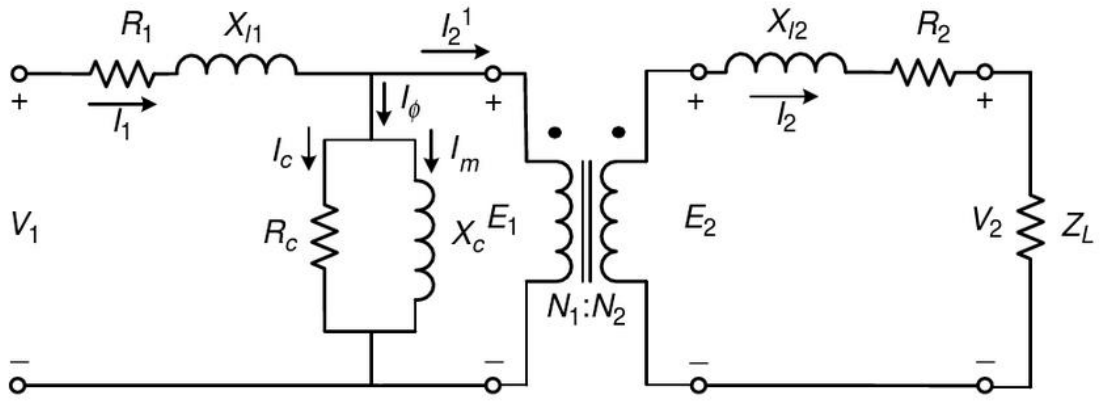

Figure 3.3. Equivalent circuit of the practical transformer. Image is taken from reference [25].

Where R1, Xl1 is the equivalent impedance of the primary winding, R2, Xl2 are the equivalent impedance of the secondary winding, Xc is the mutual inductance.

Ferrite cores are used in power electronic applications when operating at high frequency. Based on the resistance of the magnetic material, ferrites are divided into hard ferrites and soft ferrites. Hard ferrites are otherwise known as permanent magnets. They are made of iron oxide, barium carbonate and strontium carbonate. These ferrites have high coercivity and remanence after magnetization. Coercivity defines resistance of the material to change in its magnetic flux and remanence defines the material's ability to have magnetic flux after removing the applied external

magnetic field. Therefore, hard ferrites are hard to magnetize and demagnetize. Applications of hard ferrites are magnetic discs, microwave filters, magnetic tapes and electric motors. In contrast, soft ferrites are not permanent magnets. They are made of nickel, zinc and manganese. Soft ferrites have low coercivity and hence these materials have the ability to magnetize in reverse direction by releasing less energy which is called the hysteresis loss. These materials dissipate low losses at high frequencies. Therefore, soft ferrite based core material was selected for the transformer core.

A wide variety of ferrite core shapes and materials are available. Some of the different ferrite core shapes can be seen in Figure 3.4 [26].

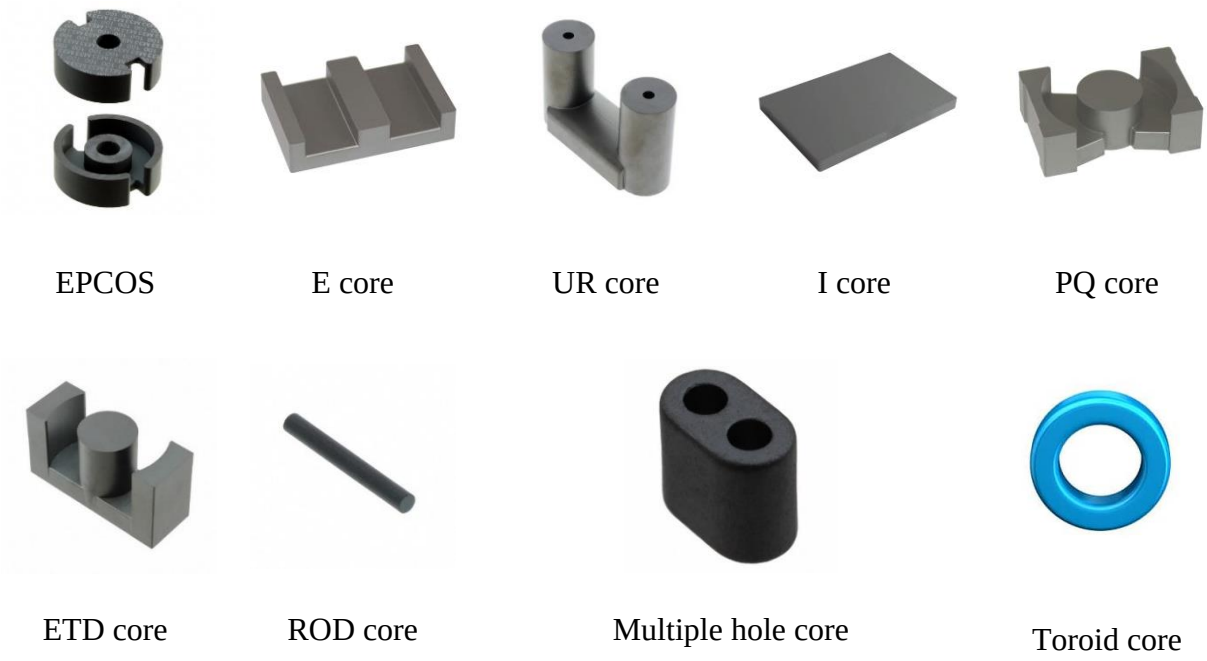

Figure 3.4. Different ferrite core shapes. Images are taken from reference [26].

Two different core shapes can be placed together to form a transformer with air gap. Some of the examples are shown in Figure 3.5.

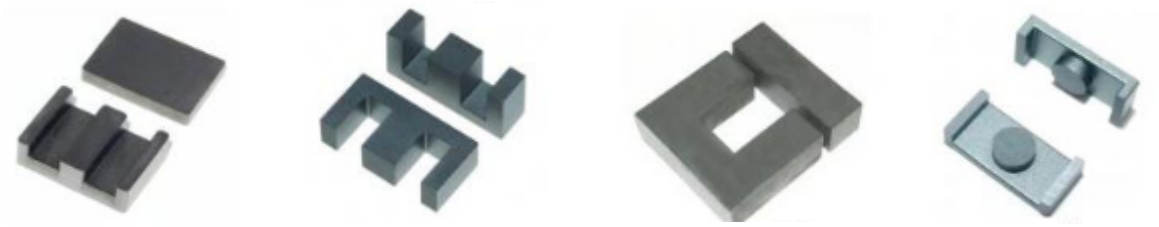

EI core EE core UI core EER core

Figure 3.5. Different core shapes for transformer

Comparatively, benefits of toroid cores overshadow their drawbacks. Toroid cores have higher efficiencies because of its higher flux density. Due to its closed structure, most of the magnetic field is contained and so lower magnetic field is emitted from the core. Toroid core structure has no air gap, which avoids leaking of magnetic flux to external components that are placed adjacent to it [24].

Toroid core is donut shaped which gives an advantage of using the single turn high voltage insulated hook up wire and enabling the possibility of using a single inverter to generate multiple outputs. The closed structure of the core gives the benefit of low leakage inductance since most of its magnetic flux is confined inside the core.

Core material can be picked based on operating frequency, core losses, flux density at the operating frequency, magnetic field strength (B-H graphs) and permeability or permittivity. Every manufacture classify ferrite cores based on different parameters with different nomenclature. Ferroxcube has analyzed different materials available for different core types and sizes [27]. For example magnetics manufacturer has classified ferrite cores, as shown in Figure 3.6, including materials such as initial permeability, maximum operating frequency, loss factor relative to other materials at room temperature, temperature, flux density at room temperature, power loss, resistivity and density [28].

			INDUCTORS & POWER TRANSFORMERS					EMI/RFI FILTERS & BROADBAND TRANSFORMERS			LINEAR FILTERS & SENSORS		
MATERIAL			L	R	P	F	T	J	W	M	C	E	V
Initial Permeability	μ_i		900 ±25%	2,300 ±25%	2,500 ±25%	3,000 ±20%	3,000 ±25%	5,000 ±20%	10,000 ±30%	15,000 ±30%	900 ±25%	2,000 ±25%	2,300 ±25%
Maximum Usable Frequency (50% roll-off)	f	MHz	≤6	≤1.8	≤1.8	≤1.5	≤1.5	≤0.7	≤0.5	≤0.12	≤8	≤3	≤1.5
Relative Loss Factor X 10^{-6} 25°C		tan δ/μ_{ac}						≤15 100 kHz	≤7 10 kHz	≤10 10 kHz	≤10 300 kHz	≤3 100 kHz	≤5 100 kHz
Curie Temperature	T_c	°C	>300	>210	>210	>210	>220	>145	>135	>130	> 200	>160	>170
Flux Density @ 1,194 A/m (15 Oe) 25°C	B_m 10 kHz	G mT	4,200 420	4,700 470	4,700 470	4,700 470	5,300 530	4,300 430	3,900 390	4,700 470	3,800 380	3,600 360	4,400 440
Remanence 25°C	B_r	G mT	1,500 150	1,600 160	1,600 160	1,500 150	1,500 150	1,000 100	800 80	2,700 270	1,500 150	700 70	1,500 150
Power Loss (PL) Sine Wave in mW/cm³ (typical)	25 kHz 200 mT (2,000 G)	@25°C		90	180	60	80						
		@60°C		65	110	55	75						
		@100°C		60	65	90	70						
		@120°C		65	110	125	75						
	100 kHz 100 mT (1,000 G)	@25°C		87	70	70	65						
		@60°C		64	50	65	57						
		@100°C		58	65	110	55						
		@120°C		64	45	150	58						
	500 kHz 50 mT (500 G)	@25°C	290										
		@60°C	150										
		@100°C	115	175	300		150						
		@120°C	130										
Resistivity	ρ	Ω-m	10	5	5	5	5	0.5	0.1	0.5	2	2	1
Density	δ	g/cm³	4.8	4.8	4.8	4.8	4.8	4.8	4.9	5.0	4.7	4.7	4.8

Figure 3. 6. Magnetics material classification. Image is taken from reference [28].

3.2. High voltage isolation design

As mentioned in section 1.2, high voltage isolation design can be obtained by different kinds of transformer techniques such as wireless power transfer, power over fiber, and planar transformers. When designing a multiple output power supply, these techniques need a primary inverter for every output that is generated. Wireless power transfer, optical fiber and planar transformers were not considered as it contrasts the small size design of the power supply. To achieve high voltage isolation, a core with a large size has to be considered to satisfy the creepage

and clearance of the transformer. Creepage is measured as the shortest distance between two conductors through the insulated path. Clearance is defined as shortest distance between two conductors through air. Refer to Figure 3.7 [29] for clearance and creepage path of the toroidal transformer.

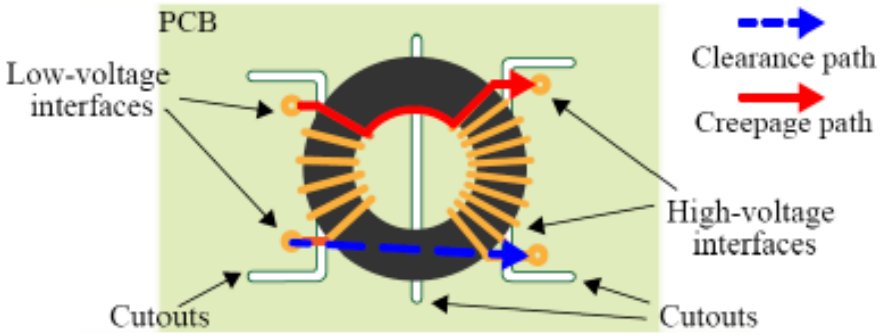

Figure 3.7. Creepage and clearance path for toroid core with 2 windings. Image is taken from reference [29].

In the implemented design, a single turn primary winding was used across all the toroid cores connected to the primary inverter. A high voltage insulated hook up wire was used as a single turn primary winding, which has an insulation material surrounded by a conductor. Therefore, the creepage distance can be satisfied by varying the length of the high voltage insulated hook up wire, and the clearance distance is satisfied by placing the primary and secondary inverters on different PCB's. A high voltage insulated hook up wire - 20SRT30 cable was considered for the single turn primary winding. This cable has silicon rubber as the insulation material and an insulation voltage of upto 30 kVDC.

A smaller toroid core size was preferred to satisfy the clearance and creepage distances. Refer to Figure 3.8 for clearance and creepage path of the toroidal transformer with a single turn primary winding.

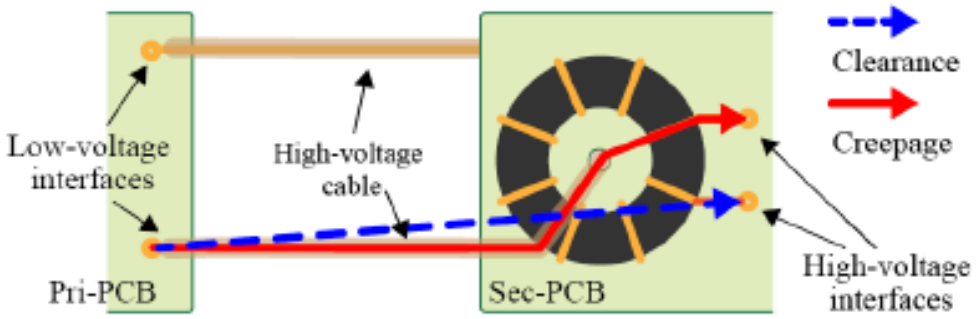

Figure 3.8. Creepage and clearance path for toroid transformer with single turn primary winding. Image is taken from reference [29].

3.3. Limiting common mode current

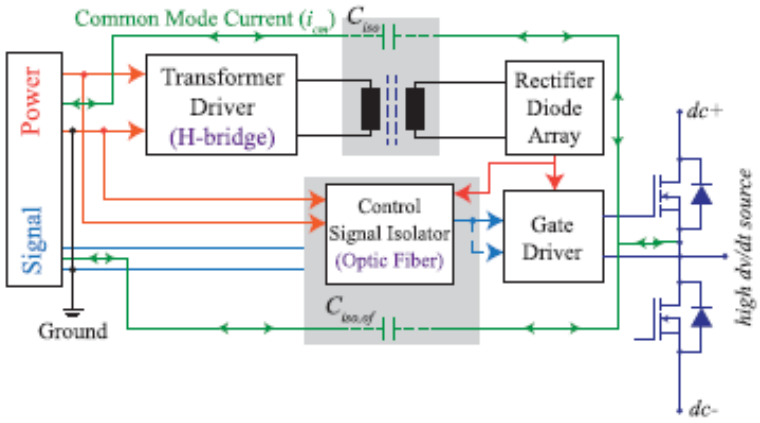

Figure 3.9. Common mode current path. Image is taken from reference [30]

Power devices switch at very high speeds (fast switching), so it is important to limit common-mode current across the devices. Common mode current path in a half bridge module is seen in Figure 3.9. For high switching operations, a very low coupling capacitance is required across the transformer. Kadavelugu and Bhattacharya reported a study which clearly demonstrated that in case of failure to limit the common mode current, high *dv/dt* in the module will distress the gate driver control signals resulting in a continuous voltage stress in the gate driver which leads to

reduced lifetime of the isolation stage [31]. Common mode current can be calculated by the following equation,

$$i_{CM} = C_{Coupling} * \frac{dv}{dt}$$

where, i_{CM} is the common mode current, $C_{coupling}$ is the coupling capacitance across the gate driver power supply, *dv/dt* is the switching voltage of the SiC MOSFET.

The power devices rated beyond 10kV have very high *dv/dt* (30 *kV/µs* – 100 *kV/µs*) [9] at switching periods. These high switching transients passes high frequency currents to the gate driver control circuits. For example when switching at 100 *kV/µs* with transformer coupling capacitance, C_{XMER}, of 5 pF generates a peak current of 500 mA. This current has a return path flowing through control signals and power supply circuits. These high frequency currents when passing through interconnecting impedances give rise to voltage spikes which damages the operation of controller circuit along with converter circuits. Therefore, in order to limit the common-mode current, a very low coupling capacitance is required (< 5 pF). Considering the single input multiple output power supply design, transformer coupling capacitance is set to be < 1 pF [32]. The transformer coupling capacitance, C_{XMER}, afforded due to the physical structure of the transformer is cylindrical as illustrated in Figure 3.10.

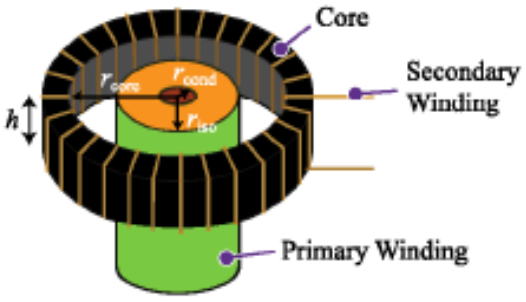

Figure 3.10. Capacitor model of the toroid transformer. Image is taken from reference [32].

The theoretical coupling capacitance of the transformer can be calculated based on the capacitor model of the toroid transformer [30] as

$$C_{XMER} = 2\pi\epsilon_0 h \left(\frac{\ln\left(\frac{r_{core}}{r_{iso}}\right)}{\epsilon_r} + \frac{\ln\left(\frac{r_{iso}}{r_{cond}}\right)}{\epsilon_{r,iso}} \right)^{-1}$$

where, h is the height of the core, r_{core} is the inner radius of the core, r_{iso} is the radius of the primary winding, r_{cond} is the radius of the primary conductor.

3.4. Dielectric strength

Partial discharge reduces lifetime of the transformer, so it is important to have a partial discharge free dielectric design. The transformer was designed in such a way that the maximum electric field around the core is less than 2 kV/mm (dielectric strength of air) to avoid using any extra material for insulation. As the primary winding is connected to the ground and secondary windings are at high potentials, the electric field distortion at the bending corner of the secondary and core is not considered. The theoretical calculation for maximum electric field is

$$E_{max} = \frac{V_{pd}}{r_{pi} \ln\left(\frac{d_1}{r_{pi}}\right)}$$

where E_{max} is the maximum electric field across the transformer, V_{pd} is the partial discharge voltage, r_{pi} is the radius of the primary winding, d_1 is the distance between inner radius of core and center of the core.

To achieve an air insulated design, Emax margin was set at 2 kV/mm including the tolerance. Additionally, a 3D printed support box, as depicted in Figure 3.11, was designed using the solidwork 2020 application to make sure that the single turn primary winding (high voltage insulated hook up wire) stays at the center of the core. This will prevent unwanted influence on the electric field or flux density due to the nearest secondary winding turns [18].

Figure 3.11. 3D printed support box.

3.5. Saturation evaluation

Some of the properties to consider when making trade-offs for saturation evaluation would be permeability, saturation flux density, and core losses.

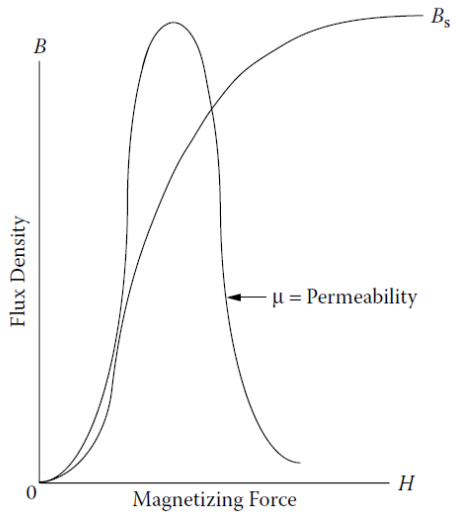

Figure 3.12. Variation of permeability in B-H loop. Image is taken from reference [25].

Permeability of a material is its ability to magnetize when magnetic field is applied. Mathematically, permeability, μ is defined as the ratio of flux density, B to magnetizing force, H.

$$\mu = \frac{B}{H}$$

The variation of the permeability in B-H plot is shown in Figure 3.12 [25].

The B-H or hysteresis loop of a soft magnetic material is seen in Figure 3.13 [25]. Saturation point is referred as the highest point in the B-H plot where any further increase in magnetic field strength does not provide any useful flux density. The magnetizing force at the saturation point is referred as H_s and the flux density at the saturation point is referred to as B_s are shown in the Figure 3.13 with dashed lines.

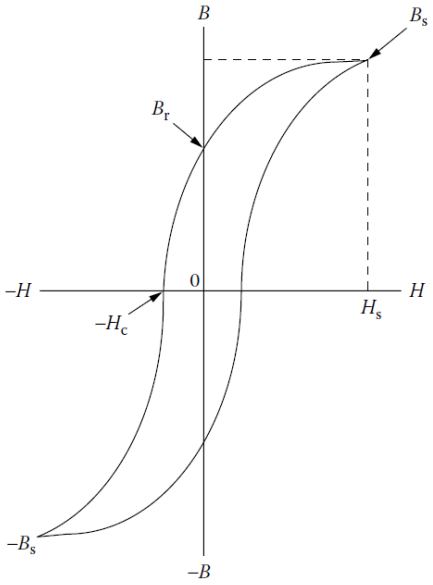

Figure 3.13. Hysteresis loop of a soft magnetic material. Image is taken from reference [25].

The area enclosed in the hysteresis of the plot in Figure 3.13 is the degree of energy loss in the material. This loss consists of hysteresis loss and eddy current loss. When flux is passed through the core, an EMF is induced in the material resulting in currents to circulate inside the material. These circulating currents are the eddy currents and the losses due to eddy currents are called eddy current losses. Core losses can be estimated by the Steinmetz equation [33].

$$\rho_v = k f_s^{\alpha} \Delta B^{\beta}$$

where, ρ_v is volumetric losses, f_s is the switching frequency, ΔB is the flux density.

The material with high electrical resistance produces low current resulting in low eddy current losses. Therefore, one of the ways to mitigate the core losses would be selecting a core material with high resistivity and operating in its limitations to prevent the core from overheating.

3.6. Selection of core size

By considering the maximum electric field and coupling capacitance, size of the core was calculated using the MATLAB software. As discussed in 3.4., E_{max} is considered as 2 kV/mm in order to achieve the air insulated design of the core and the partial discharge voltage is estimated to be 16 kV for MV active gate driver. The MATLAB simulation result can be seen in Figure 3.14. According to plot in Figure 3.14, for the selected partial discharge voltage, E_{max} and the high voltage insulated hook up wire, the inner radius of the core is limited to 15.52 mm.

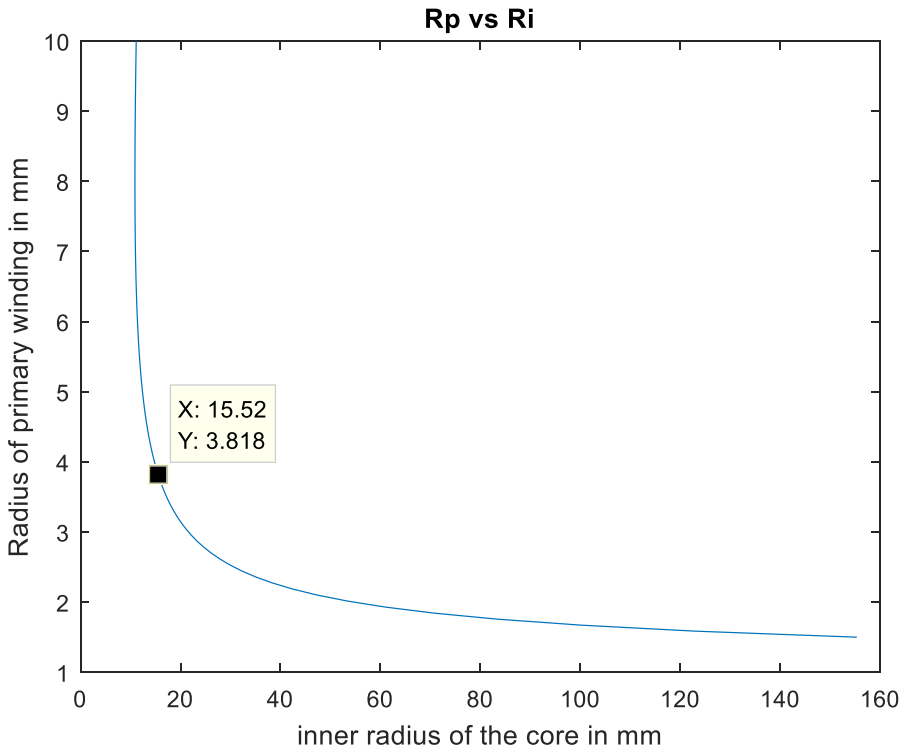

Figure 3.14. Inner radius of core selection

As discussed in section 3.3., the equation of the coupling capacitance is used to calculate the height of the core. The design target of the coupling capacitance is considered to be < 1 pF. The given permittivity of free space is 8.825e-3 pF/mm, permittivity of air is 1.0006, and permittivity of isolator (silicon rubber) is 3.9. The MATLAB simulation result can be seen in Figure 3.15. According to the plot, the selection of height of the core is limited to 19.81 mm.

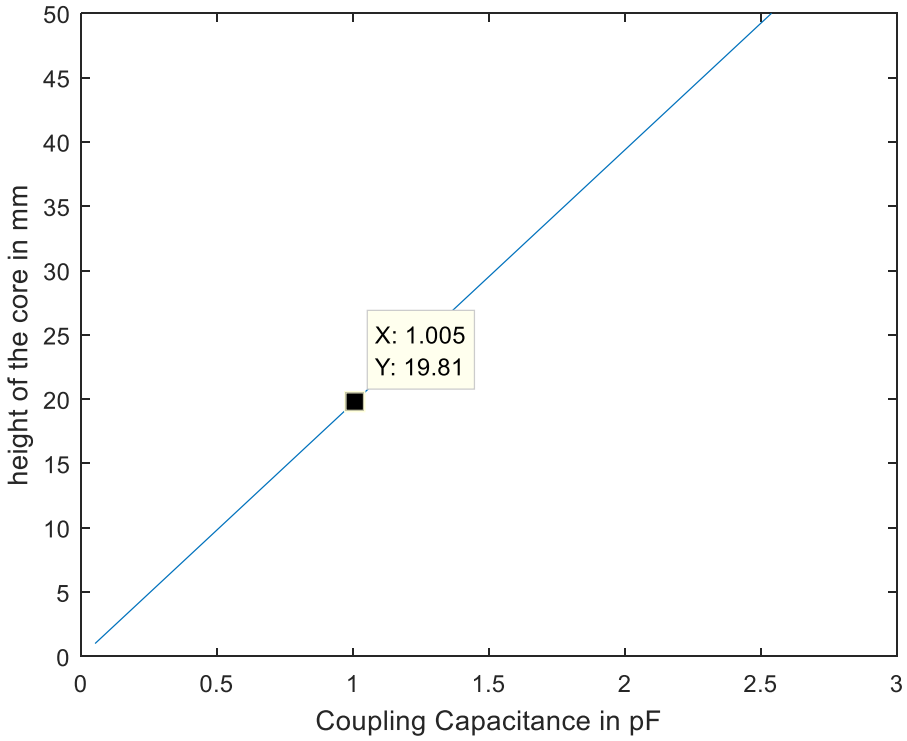

Figure 3.15. Height vs coupling capacitance of the core.

With the inner radius of core and height of the core determined, core size is selected as 41.8mmx26.2mmx18mm among the available core sizes. 41.8mm is the outer diameter, 26.2mm is the inner diameter and 18mm is the height of the core as seen in Figure 3.16.

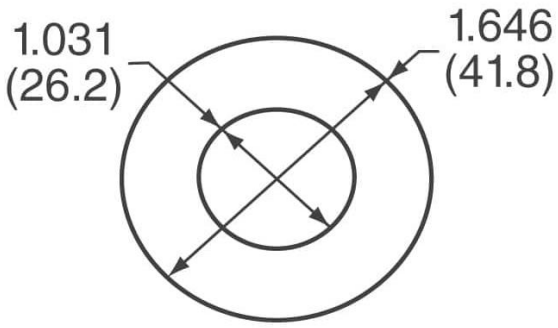

Figure 3.16. Dimensions of the selected toroid core

For the core size 41.8mmx26.2mmx18mm, the available ferrite materials are 3C90, 3C94, 3E27, N87, N30, T65, T38 and T35. 3C90 and 3C94 are ferrite material whereas the remaining materials are of silicon ferrite (Si Fe) material. Maximum operating frequency for materials 3C90 and 3C94 are 200kHz and 300 kHz respectively. Whereas, operating frequency range for 3E27 material was not mentioned in the datasheet. T38 material's frequency varies from 10kHz to 100kHz. For materials T65 and T35, frequency ranges between 10kHz and 200kHz. For material N87 frequency domain is 25kHz to 500kHz. Material N87 is more suitable for the chosen core size as the switching frequency is 500kHz.

To evaluate the number of turns at the secondary winding, gauss law of magnetism was used as follows,

$$B_{max} = \frac{V_o * D * T_s}{2 * A_c * N_s}$$

where, V_o is the output voltage, D is the duty cycle, T_s is the switching time period, A_c is the cross sectional area of the core and N_s is the number of turns at secondary windings.

For the core material N87, maximum flux density operating at 500kHz is 250 mT. Duty cycle was considered to be 0.5. Using these parameters, secondary number of turns were plotted with maximum flux density in MATLAB as shown in Figure 3.17. The nearest integral number is taken as the number of turns below 250 mT of flux density. Therefore, number of turns for

secondary windings is calculated as 3 while number of turns at primary windings is 1. Based on the simulation results and design considerations, all the parameters of the designed core are illustrated in Table 5.

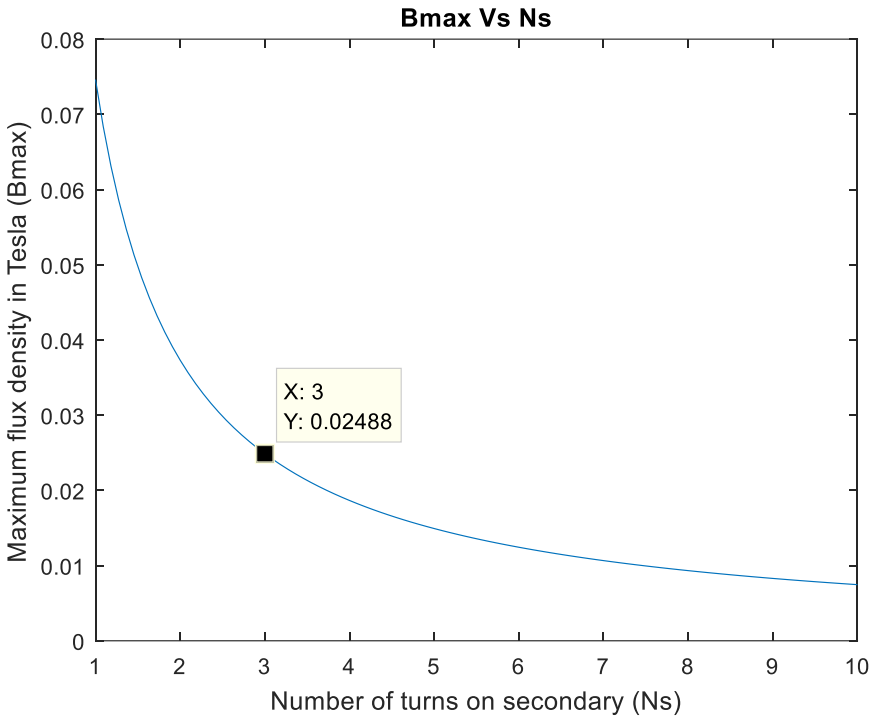

Figure 3.17. Maximum flux density to number of turns calculation

Table 5. Designed core specifications

Frequency range	25 kHz – 500 kHz
Material name	Si Ferrite
Material code	N 87
Size of the core	41.8x26.2x18

3.7. Simulation

For simulation of the toroid transformer, " Solidworks 2020" and "ANSYS Electronic Desktop" were used. The 3D model of the toroid core and secondary windings were designed in

the “Solidworks 2020” application then imported into “ANSYS Electronic Desktop” application. When the 3D design of the toroid transformer was designed in the solidworks application and it was saved as the step file (“.stp” extension file). Then it was opened in the ANSYS application and a new project was created in “Q3D design extractor”, the step file was imported and then design the primary winding to complete the transformer design. Figures 3.18 & 3.19 depict screenshots of 3D design transformer model from Solidworks and ANSYS applications.

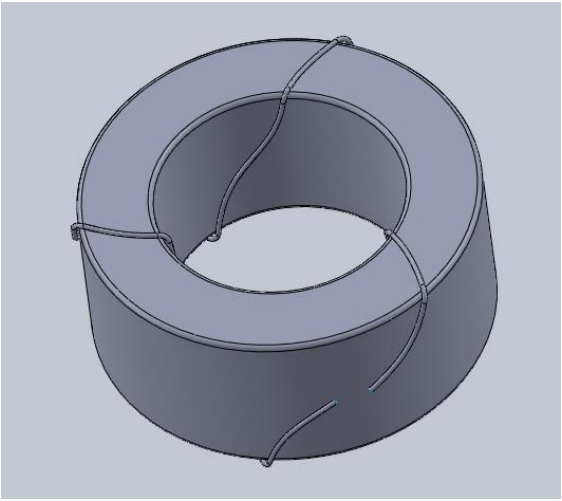

Figure 3.18. Screenshot of 3D design of transformer from solidworks software application

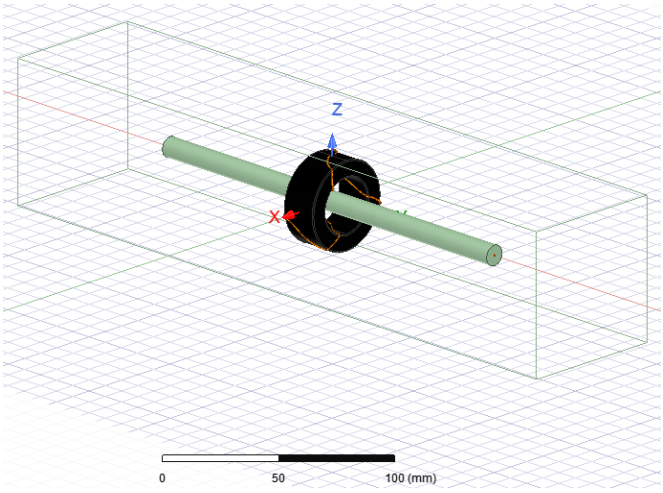

Figure 3.19. Screenshot of 3D design of transformer from ANSYS software application

In ANSYS software, primary winding and secondary winding are referred as nets. Each net has source and sink terminals to define the current paths in the conductors, where source terminal was defined as existed potential or current flow entering and the sink terminal was defined as zero potential or current flow exiting the conductor. The source and sink terminals were given for both the primary and secondary windings, followed by defining the solution setup to run the simulation. The matrix report was created to read the values of inductance and capacitance of the toroid transformer. Results of the ANSYS simulation are illustrated in the below Table 6.

Table 6. Simulation results of ANSYS Q3D design

Parameter	**Value**
Leakage inductance	1.682850 uH
Secondary self inductance	4.225100 uH
Mutual inductnace	12.660016 uH
Coupling co-efficient	0.8874

A new project was created in “Maxwell 3D”, where solution type was selected as “electrostatic” to read the electric field. The simulation setup for Maxwell 3D is similar to Q3D except for defining the nets. In Maxwell 3D, excitations were given to the conductors instead of source-sink terminals. Electric field simulation results are depicted in Figure 3.20.

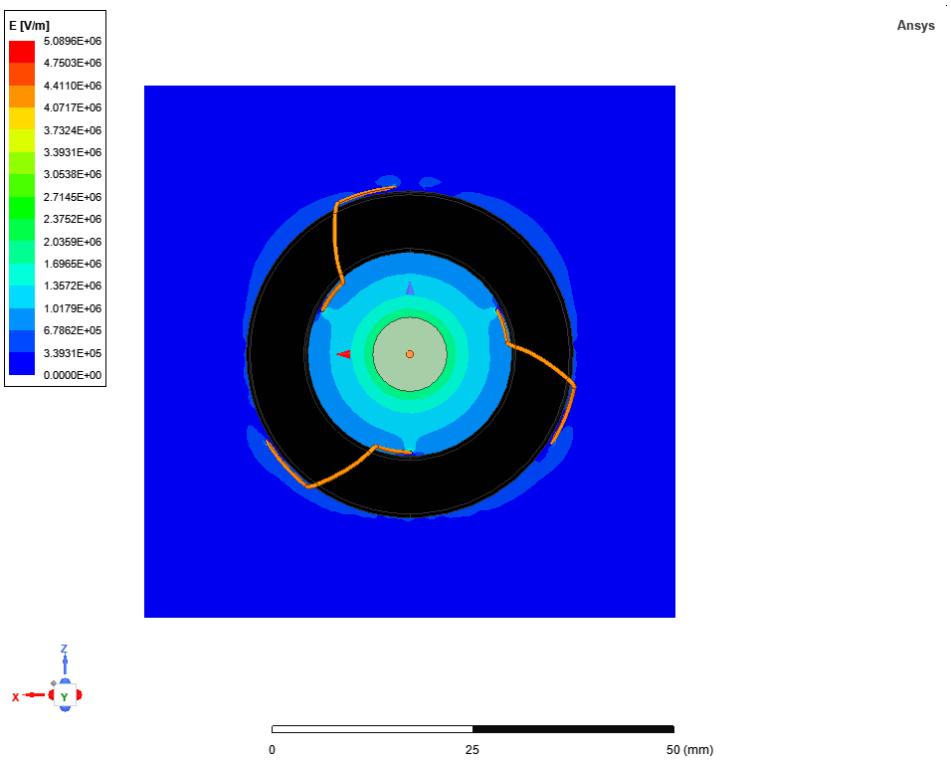

Figure 3.20. Electric field simulation in ANSYS.

The value of the electric field is represented in gradiation of color as depicted on the left in Figure 3.20. According to simulation results, an electric field strength of about 1.70 kV/mm – 2.04 kV/mm was seen between the primary winding and the inner radius of the core which matched with the design consideration of the core. Thus, air insulated design was achieved.

CHAPTER 4

EXPERIMENTAL RESULTS

4.1. Test prototype

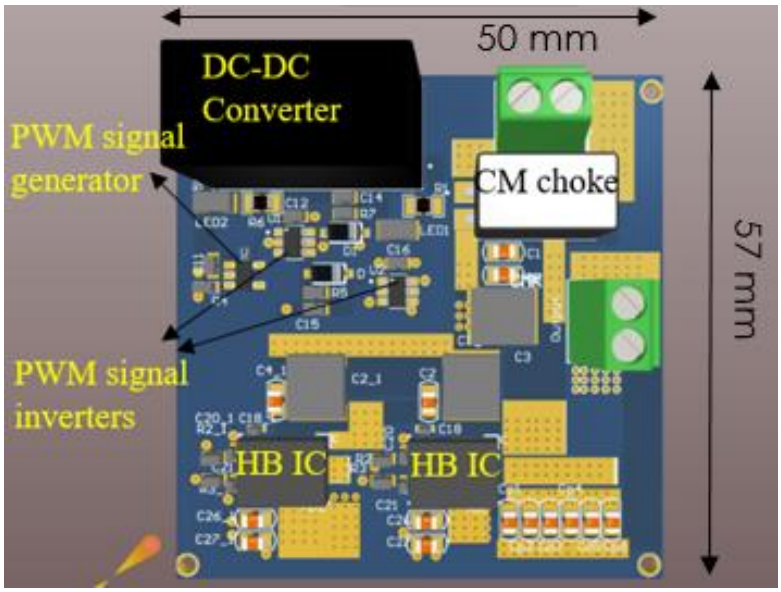

Figure 4.1. Primary inverter

The primary and secondary inverters of the power supply are shown in Figures 4.1 & 4.2. In the designed power supply, a common mode (CM) choke is used to filter out the noise from input signal. A DC – DC converter was used as a power supply to generate an output voltage of +5 V and this +5 V was given to the half bridge integrated circuit (IC), PWM generator and PWM generator signal inverting ICs (dual schmitt trigger inverters). To generate the PWM signal, IC, "TC1799IS5TRMPBF" was used. The frequency, 1 kHz to 33 MHz, was determined by the resistor and its corresponding "R_{SET}" values range from 3 kΩ to 1 MΩ. Two half bridge ICs named "LMG5200" were used to form a full bridge circuit. Some of the key features of half – bridge IC are capability of switching upto 10 MHz, undervoltage lockout protection, low power consumption, good propogation delay of 29.5 ns and 2ns of matching. The dual schmitt trigger

inverter ICs named “SN74LVC2G14DBVR” were used to invert the PWM signals and were given to the half – bridge ICs.

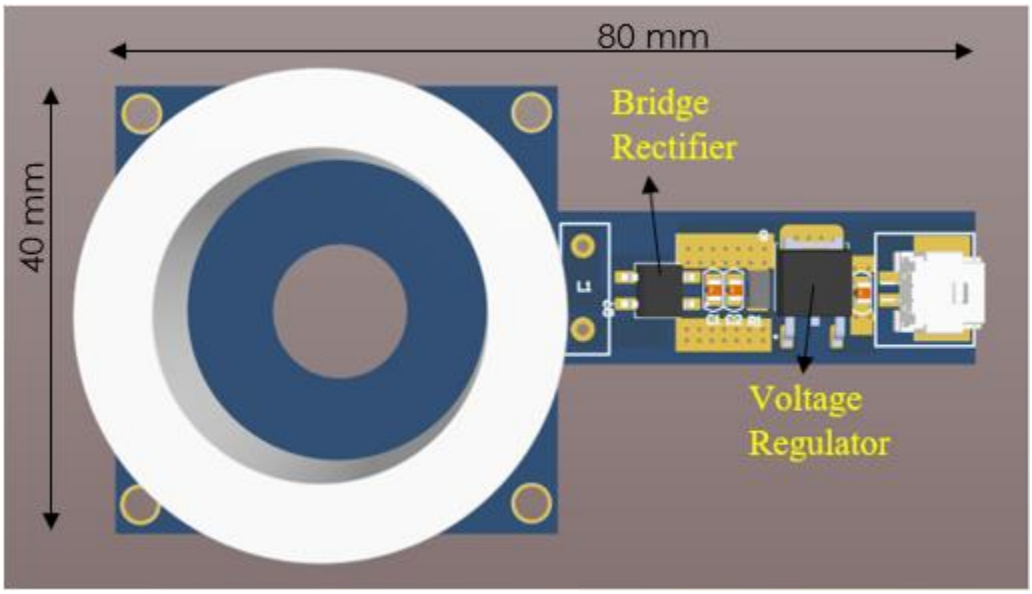

Figure 4.2. Secondary inverter

In the secondary circuit, a bridge rectifier named “MB10S-13” was used which had an internal structure of full bridge diode rectifier. Some of the key features of bridge rectifier are miniature package which helps with saving space on PCB board, low leakage current and low forward voltage drop. Lastly, a voltage regulator was used to regulate the output voltage. Component specifications of the designed power supply are listed in Table 7.

Table 7. Component specifications of the power supply

Component	**Name**
PWM generator	TC1799IS5TRMPBF
Dual Schmitt trigger inverter	SN74LVC2G14DBVR
Half Bridge IC	LMG5200
Diode bridge rectifier	MB10S-13
Voltage regulator	LM7805CT

4.2. Parameter extraction

"Keysight impedance analyser E4990A 20 Hz – 30 MHz" was used to verify the coupling coefficient, leakage inductance and mutual inductance of all the three cores. To calculate the leakage inductance across all the 3 cores, all the secondary windings were shorted and the leakage inductance was seen across the primary winding i.e., high voltage insulated hook up wire. To calculate the mutual inductance across all the 3 cores, all the secondary windings were open circuited and the mutual inductance was seen across the primary winding i.e., high voltage insulated hook up wire. Resonant capacitance was calculated based on the mutual inductance across all the 3 cores. The same test set-up procedure was used to measure the mutual inductance and leakage inductance across the single core. The impedance analyser setup is depicted in Figure 4.3 and snapshot of leakage inductance across all the 3 cores in impedance analyzer is shown in Figure 4.4.

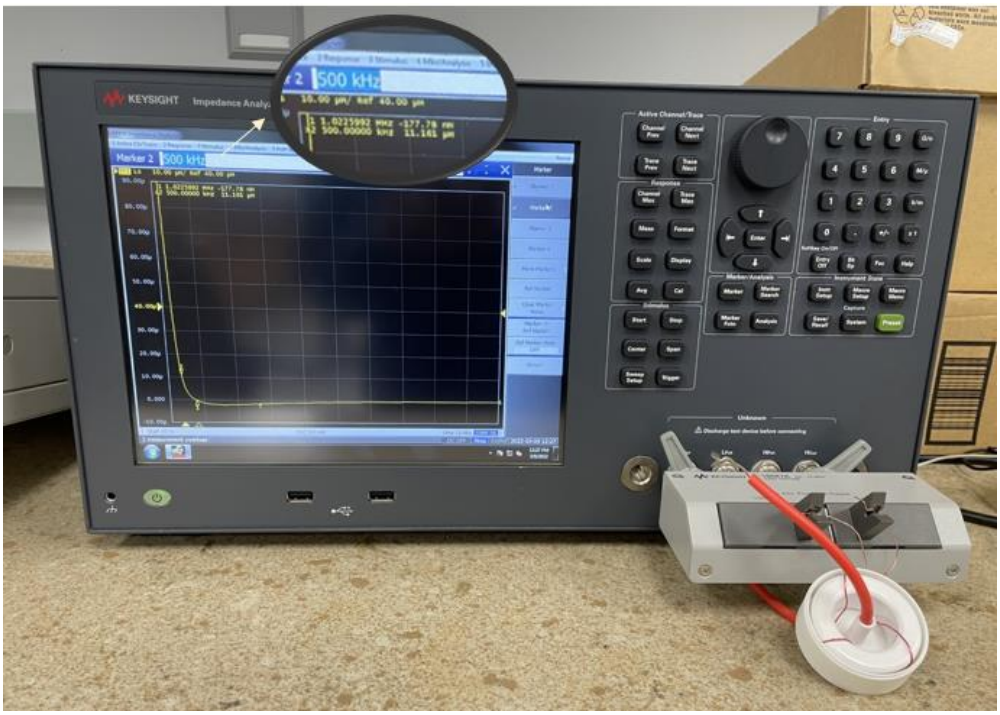

Figure 4.3. Impedence analyser setup to read mutual inductance for single core

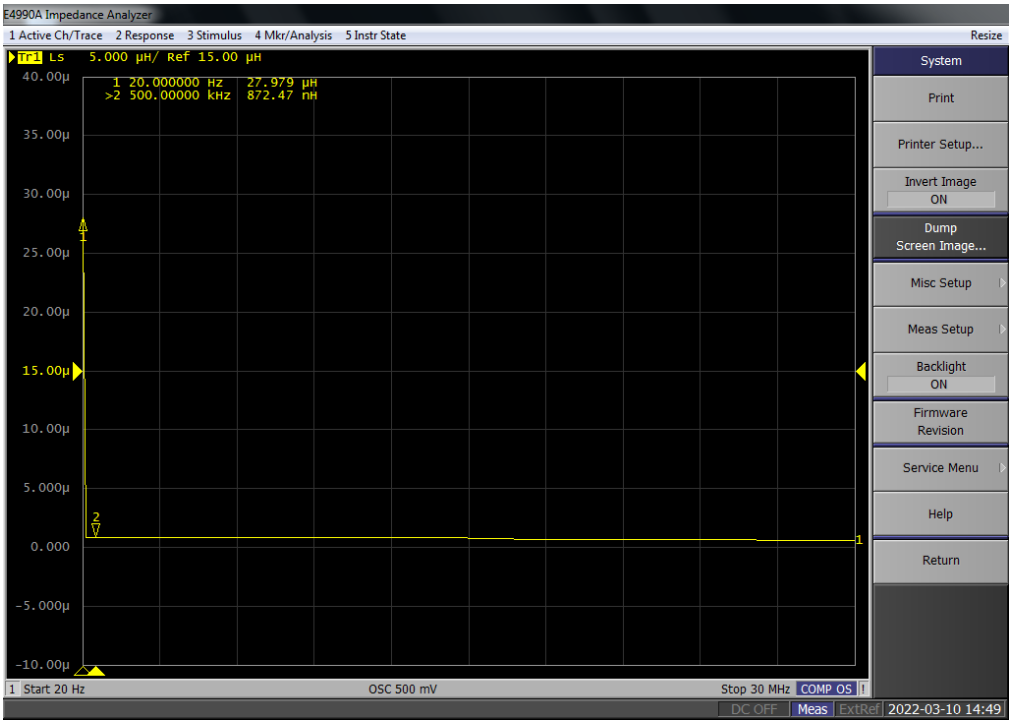

Figure 4.4. Snapshot of impedance analyzer to measure leakage inductance

The mutual inductance and leakage inductances for single core and across all the 3 cores that were recorded from the impedance analyzer are listed in Table 8. The mutual and leakage inductance are approximately similar compared to simulation results in Table 5.

Table 8. Readings from the impedance analyser

Type of inductance	Inductance (uH)
Mutual inductance for Core 1	11.141
Mutual inductance for Core 2	11.337
Mutual inductance for Core 3	9.461
Mutual inductance for all 3 Cores	3.074
Leakage inductance for all 3 Cores	0.872

4.3. Output voltage verification

In the Figure 4.5, input voltage was given from the DC power supply and output voltages across all the 3 loads were measured using the multi-meter. Input was given to the primary inverter and the single turn primary winding was connected to the primary inverter through all the 3 cores. The secondary windings of the cores were connected parallelly to the voltage regulator and resistive load.

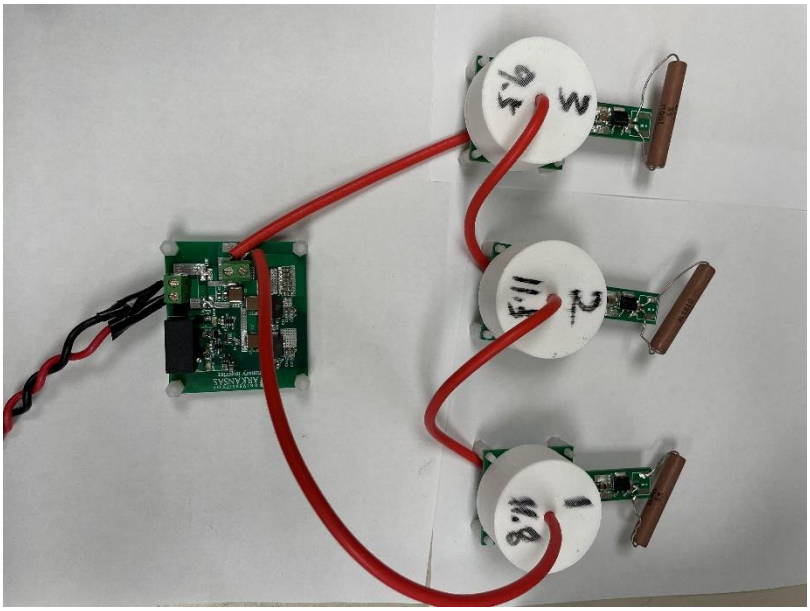

Figure 4.5. Experiment test prototype

Input was given as 20 V. 1 A from the power supply was given to the primary converter with a balanced resistive load of 100 ohm to all 3 secondary cicuits. Output voltage and power were measured across all the 3 secondary circuits along with their respective magnetizing inductance. These values are listed in Table 9. The efficiency of the single-input three-output power supply was calculated to be around 48%.

The output voltage for all 3 secondary converters when compared to the LTSpice simulation results in Table 4 are acceptable within error limitation since the LTSpice simulations are performed on the ideal cases.

Table 9. Magnetising inductance and output volatge for all 3 cores

	Magnetizing inductance (uH)	Output voltage (V)	Output Power (W)
Core 1	11.870	18.76	3.52
Core 2	11.337	17.8	3.16
Core 3	9.461	17.25	2.97

4.4. DC insulation test

The insulation test setup of the transformer is depicted in Figure 4.6. The common way of doing the DC insulation test for a device is applying twice the switching voltage of the module. For the DC insulation test of the transformer, ground potential was given to the primary winding and partial discharge voltage difference was given at the secondary winding from the high volatge DC power supply. The designed transformer had insulation voltage or partial discharge voltage of about 20 kV. In case of failure, i.e., if the device cannot handle the applied partial discharge voltage, the device would emit the eletrical sparks or make noise. When the transformer was subjected to voltage higher than 20 kV, a humming noise was observed. The insulation voltage of 20 kV was achieved for the transformer.

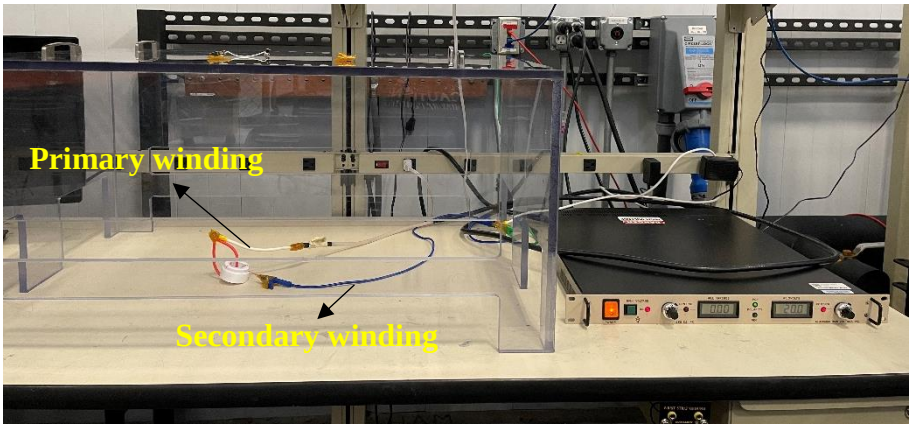

Figure 4.6. Insulation test setup

4.5. Double pulse test (DPT)

The DC input was given from the power supply to the primary inverter. The outputs from the power supply were given to high side gate driver, low side gate driver and a resistive load. The high side and low side gate drivers were connected to the top and bottom switches of the module respectively. The switching performance of the device was evaluated through the clamped inductive load. The double pulse test set up circuit diagram is depicted in Figure 4.7.

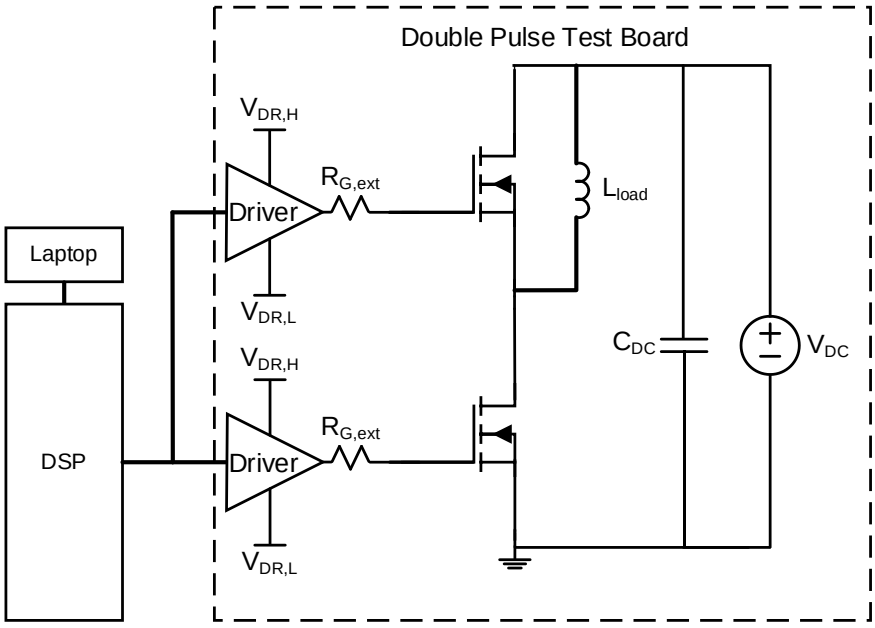

Figure 4.7. DPT test circuit configuration

The main focus of the double pulse test is to calculate the coupling capacitance of the gate driver power supply. The signals of interest would be drain-source voltage of device under test, the overshoot - rising/falling slew rate, i.e. *dv/dt*, rising duration of V_{ds} and common mode current, that comes from the gate driver power supply. The double pulse test set up is depicted in Figure 4.8.

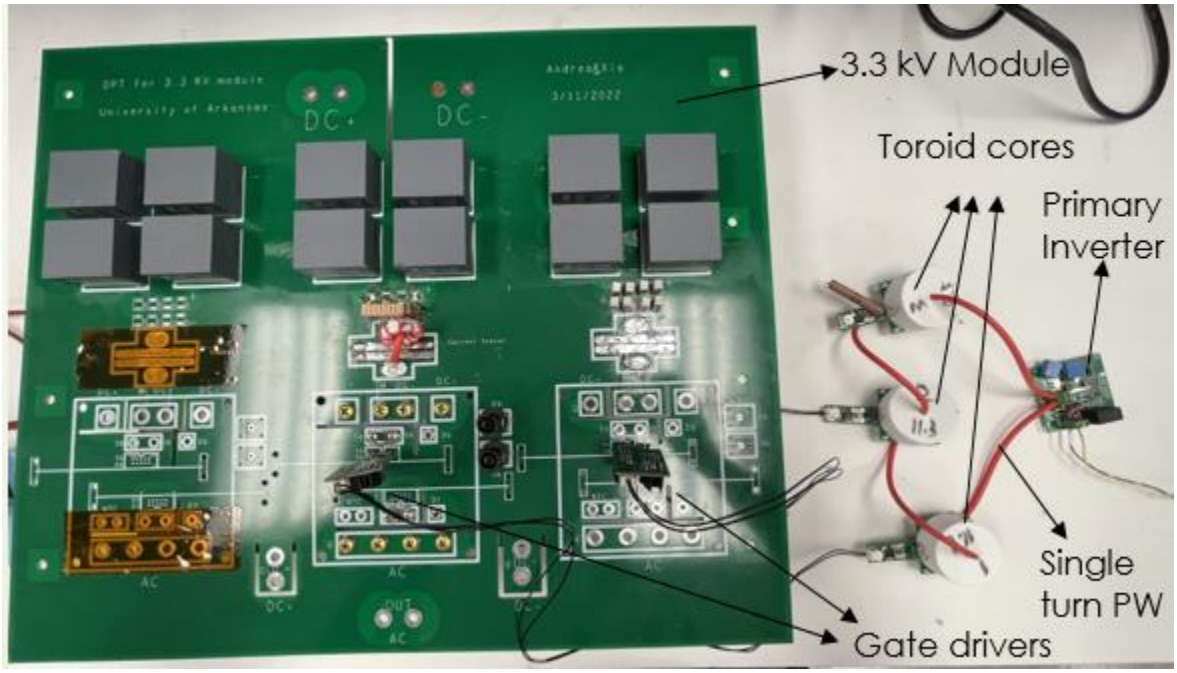

Figure 4.8. DPT test setup

The double pulse test results are depicted in Figure 4.9. The turn ON *dv/dt* is 29.34 V/ns, CM current is 84.81 mA and the equivalent coupling capacitance is 2.89 pF. The turn OFF *dv/dt* is 34.04 V/ns, CM current is 114.3 mA and the equivalent coupling capacitance is 3.35 pF.

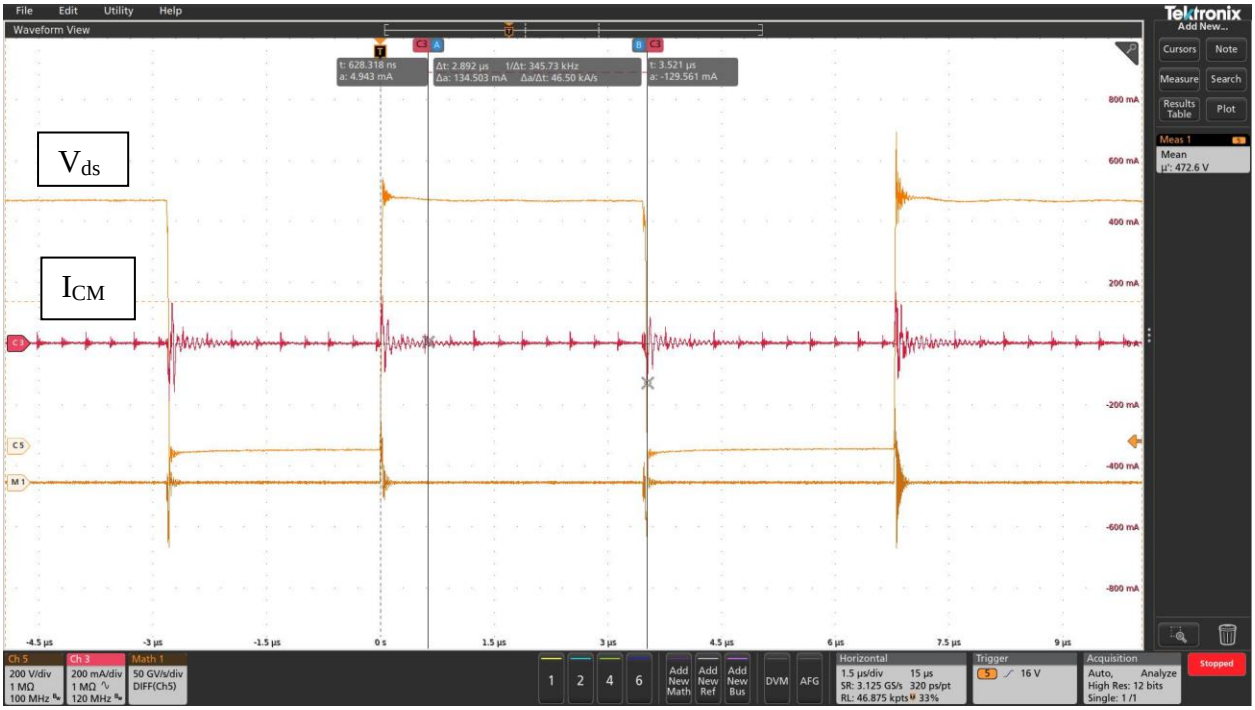

Figure 4.9. V_{ds} & I_{cm} when V_{gs} is 800 V.

The commercial power supply (RECOM REM6E-2424S), shown in Figure 4.10, is a single input and single output power supply has a common mode noise current of 2.84 A and the coupling capacitance is 4 pF as seen in Figure 4.11.

Figure 4.10. Commercial gate driver power supply

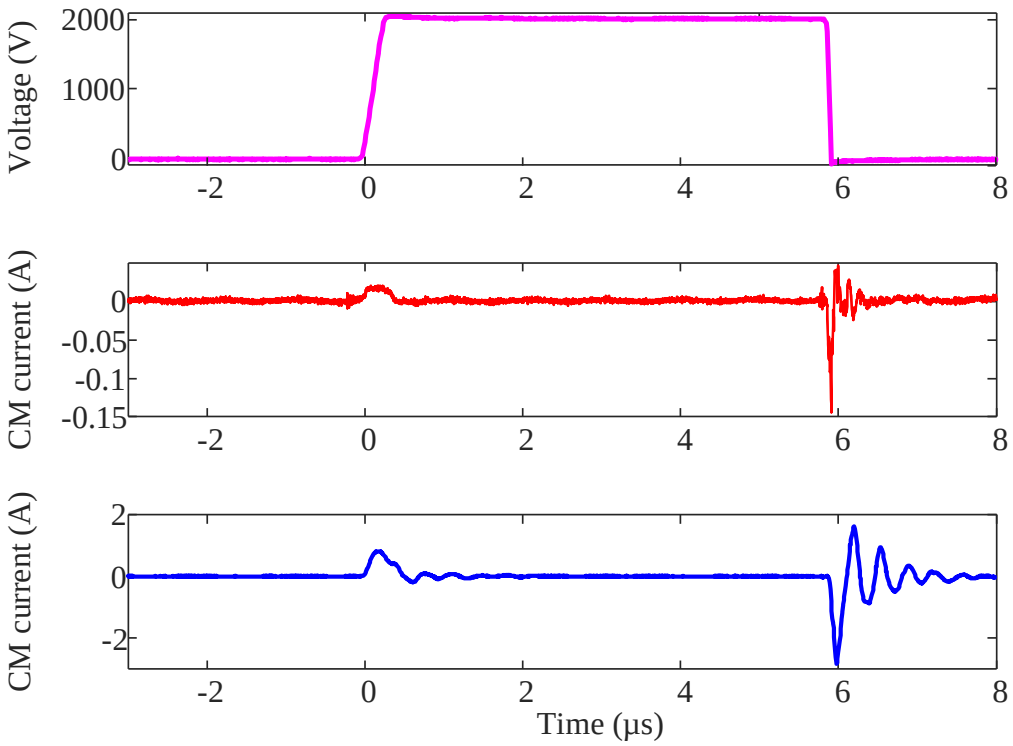

Figure 4.11. Commercial 10 kV gate driver power supply (RECOM REM6E-2424S)

In comparision designed multiple output power supply for medium voltage gate driver applications has a better coupling capacitance of around 3 pF than the commercial single input and single output power supply of 4 pF.

4.6. Thermal perfomance

In a study conducted by Yan, Dong and Burgos air insulated design of the toroid core with dimensions, 25mmx15mmx7mm in auxiliary power supply was tested to verify thermal performance and a maximum temperature of 40.6 ℃ was reported across the core as seen in Figure 4.12 [34] whereas, the proposed air insulated design generates heat around 35.5 ℃ across the core with dimensions, 41.8mmx26.2x18mm concluding that the proposed design has better thermal performance. Snapshot of thermal performance across the core is shown in Figure 4.13.

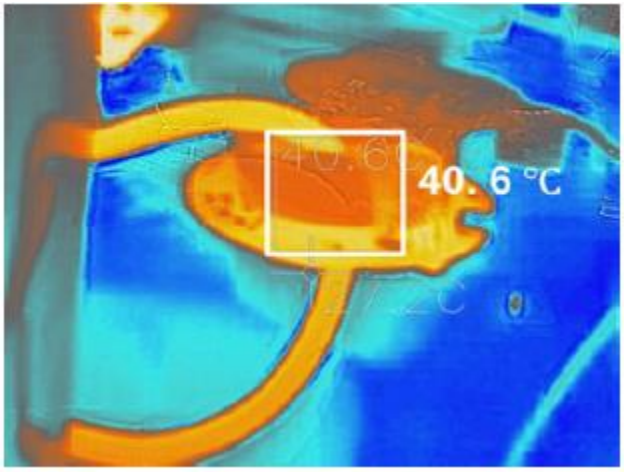

Figure 4.12. Thermal performance of air insulated design. Image was copied from reference [34].

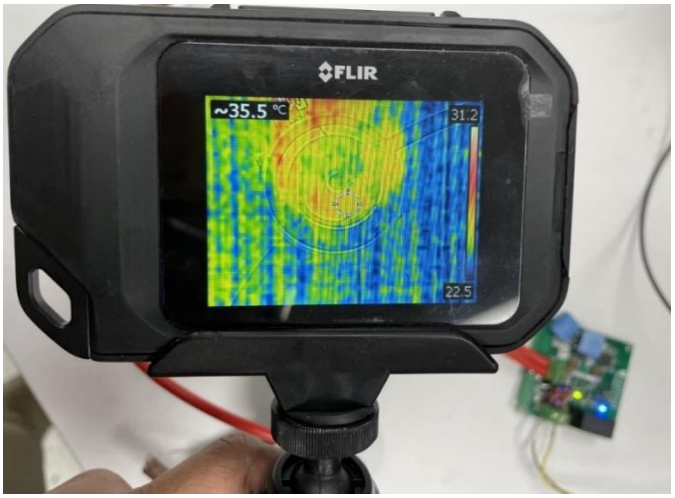

Figure 4.13. Thermal measurement of the proposed toroid core.

CHAPTER 5

SUMMARY AND CONCLUSIONS

After reviewing gate driver power supplies for medium voltage gate drivers and different isolation techniques,; different types of existing non-isolated switch-mode power supplies, their working principles, circuit flow and output waveforms; different methods to achieve isolation, their advantages and disadvantages; isolated power supply topologies to implement multiple outputs from a single input, main transformer design challenges- insulation voltage, common mode rejection current, saturation evaluation and creepage – clearance distances are considered, this thesis proposed a multiple output isolated gate driver power supply for a medium voltage gate driver where isolation is provided through high voltage insulated hook up wire using a toroidal core transformer.

Mathematical analysis was performed for the selection of core size and further FEA simulations were performed for the core to calculate the leakage inductance, mutual inductance and coupling coefficient.

An impedance analyzer was used to extract the leakage and mutual inductance parameters. These parameters were compared with the simulated results and found to be approximately similar. A DC insulation test and a double pulse test were performed for the designed core.

A comparative analysis of the coupling capacitance of the designed multiple output power supply and the commercially available single-input, single-output power supply demonstrates that the designed power supply for the MV gate driver has relatively lower coupling capacitance than the commercial power supply. The designed power supply can effectively reject the common mode current. The designed power supply can generate three outputs and has relatively smaller size with the flexibility to increase the number of outputs as required by merely changing some of the

components in the design. The isolation for the power supply is realized using the single-turn primary winding for the toroidal core transformer. The designed toroidal transformer can achieve higher insulation voltage up to 20 kV without adding any external dielectric material as the medium (i.e., air insulated design).

REFERENCES

[1] https://www.digikey.com/en/articles/use-sic-based-mosfets-to-improve-power-conversion-efficiency

[2] https://www.pntpower.com/question-really-needs-gan-sic-power-devices/

[3] Kazimierczuk, M. K. (2016). Pulse-width modulated DC-DC power converters (Second edition.). Wiley.

[4] https://www.nxp.com/docs/en/application-note/AN4833.pdf

[5] https://www.electronics-tutorials.ws/power/switch-mode-power-supply.html

[6] Ang, & Oliva, A. (2010). Power-Switching Converters, Third Edition (Third edition.). CRC Press. https://doi.org/10.1201/b12120

[7] https://training.ti.com/ti-precision-labs-isolation-what-galvanic-isolation

[8] https://atlas-scientific.com/blog/electrical-isolation-methods/

[9] https://www.allaboutcircuits.com/technical-articles/galvanic-isolation-purpose-and-methodologies/

[10] https://datasheets.maximintegrated.com/en/ds/MAX256.pdf

[11] R. Steiner, P. K. Steimer, F. Krismer and J. W. Kolar, "Contactless energy transmission for an isolated 100W gate driver supply of a medium voltage converter," *2009 35th Annual Conference of IEEE Industrial Electronics*, 2009, pp. 302-307, doi: 10.1109/IECON.2009.5414939.

[12] V. T. Nguyen and G. Gohil, "Dual-Output Isolated Gate Driver Power Supply for Medium Voltage Converters using High Frequency Wireless Power Transfer," *2020 IEEE Applied Power Electronics Conference and Exposition (APEC)*, 2020, pp. 1821-1828, doi: 10.1109/APEC39645.2020.9124146.

[13] K. Kusaka, K. Orikawa, J. -i. Itoh, K. Morita and K. Hirao, "Isolation system with wireless power transfer for multiple gate driver supplies of a medium voltage inverter," *2014 International Power Electronics Conference (IPEC-Hiroshima 2014 - ECCE ASIA)*, 2014, pp. 191-198, doi: 10.1109/IPEC.2014.6869579.

[14] X. Zhang et al., "A Gate Drive With Power Over Fiber-Based Isolated Power Supply and Comprehensive Protection Functions for 15-kV SiC MOSFET," in *IEEE Journal of Emerging and Selected Topics in Power Electronics*, vol. 4, no. 3, pp. 946-955, Sept. 2016, doi: 10.1109/JESTPE.2016.2586107.

[15] K. Mainali, S. Madhusoodhanan, A. Tripathi, K. Vechalapu, A. De and S. Bhattacharya, "Design and evaluation of isolated gate driver power supply for medium voltage converter applications," *2016 IEEE Applied Power Electronics Conference and Exposition (APEC)*, 2016, pp. 1632-1639, doi: 10.1109/APEC.2016.7468085.

[16] L. Zhang et al., "Design Considerations of High-Voltage-Insulated Gate Drive Power Supply for 10 kV SiC MOSFET in Medium-Voltage Application," *2019 IEEE Applied Power Electronics Conference and Exposition (APEC)*, 2019, pp. 425-430, doi: 10.1109/APEC.2019.8721965.

[17] N. Yan, J. Hu, J. Wang, D. Dong and R. Burgos, "Design Analysis for Current-transformer Based High-frequency Auxiliary Power Supply for SiC-based Medium Voltage Converter Systems," *2020 IEEE Applied Power Electronics Conference and Exposition (APEC)*, 2020, pp. 1390-1397, doi: 10.1109/APEC39645.2020.9124436.

[18] https://training.ti.com/ti-precision-labs-isolation-what-galvanic-isolation

[19] R. Singh, S. Bose and P. Dwivedi, "Multi-output Flyback Converter Closed loop Control with MPPT tracked PV Module," 2020 IEEE 17th India Council International Conference (INDICON), 2020, pp. 1-6, doi: 10.1109/INDICON49873.2020.9342563.

[20] Wu, Keng C.. Switch-Mode Power Converters : Design and Analysis, Elsevier Science & Technology, 2005. ProQuest Ebook Central, https://ebookcentral.proquest.com/lib/uark-ebooks/detail.action?docID=269692.

[21] K. Deepa, Padmaja PJ. and M. Vijaya Kumar, "Cascoded multi output push-pull converter," 2014 International Conference on Advances in Electrical Engineering (ICAEE), 2014, pp. 1-4, doi: 10.1109/ICAEE.2014.6838476.

[22] Y. Wei, Q. Luo and A. Mantooth, "Overview of Modulation Strategies for LLC Resonant Converter," in IEEE Transactions on Power Electronics, vol. 35, no. 10, pp. 10423-10443, Oct. 2020, doi: 10.1109/TPEL.2020.2975392.

[23] Y. Wei, Q. Luo, D. Woldegiorgis and A. Mantooth, "Multiple-Output LLC Resonant Converter with Magnetic Control," 2020 IEEE Energy Conversion Congress and Exposition (ECCE), 2020, pp. 1204-1209, doi: 10.1109/ECCE44975.2020.9235791.

[24] McLyman, Wm. T.. Transformer and Inductor Design Handbook, Taylor & Francis Group, 2011. ProQuest Ebook Central, https://ebookcentral.proquest.com/lib/uark-ebooks/detail.action?docID=1446498.

[25] Hurley, & W?lfle, W. . (2013). Transformers and Inductors for Power Electronics: Theory, Design and Applications (1. Aufl.). Wiley.

[26] https://www.digikey.com/en/products/filter/ferrite-cores/936

[27] https://www.ferroxcube.com/en-global/download/download/11

[28] https://www.mag-inc.com/Media/Magnetics/File-Library/Products/Ferrite/Magnetics-Ferrite-Materials-Web-8-17a.pdf

[29] J. Hu, J. Wang, R. Burgos, B. Wen and D. Boroyevich, "High-Density Current-Transformer-Based Gate-Drive Power Supply With Reinforced Isolation for 10-kV SiC MOSFET Modules," in *IEEE Journal of Emerging and Selected Topics in Power Electronics*, vol. 8, no. 3, pp. 2217-2226, Sept. 2020, doi: 10.1109/JESTPE.2019.2943742

[30] A. Anurag, S. Acharya, N. Kolli and S. Bhattacharya, "Gate Drivers for Medium-Voltage SiC Devices," in *IEEE Journal of Emerging and Selected Topics in Industrial Electronics*, vol. 2, no. 1, pp. 1-12, Jan. 2021, doi: 10.1109/JESTIE.2020.3039108.

[31] A. Kadavelugu and S. Bhattacharya, "Design considerations and development of gate driver for 15 kV SiC IGBT," 2014 IEEE Applied Power Electronics Conference and Exposition - APEC 2014, 2014, pp. 1494-1501, doi: 10.1109/APEC.2014.6803505.

[32] J. Gottschlich, M. Schäfer, M. Neubert and R. W. De Doncker, "A galvanically isolated gate driver with low coupling capacitance for medium voltage SiC MOSFETs," *2016 18th European Conference on Power Electronics and Applications (EPE'16 ECCE Europe)*, 2016, pp. 1-8, doi: 10.1109/EPE.2016.7695608.

[33] https://scholarworks.uark.edu/cgi/viewcontent.cgi?article=5068&context=etd

[34] N. Yan, D. Dong and R. Burgos, "A Multichannel High-Frequency Current Link Based Isolated Auxiliary Power Supply for Medium-Voltage Applications," in *IEEE Transactions on Power Electronics*, vol. 37, no. 1, pp. 674-686, Jan. 2022, doi: 10.1109/TPEL.2021.3102055.